RECRYSTALLISATION AND TEXTURE STUDIES ON 0.26 WT. PCT. P-COPPER ALLOY

By

G. V. SRINIVASAN

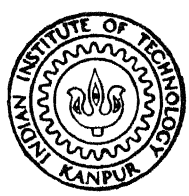

DEPARTMENT OF METALLURGICAL ENGINEERING

INDIAN INSTITUTE OF TECHNOLOGY KANPUR

DECEMBER, 1982

RECRYSTALLISATION AND TEXTURE STUDIES ON 0.26 WT. PCT. P-COPPER ALLOY

A Thesis Submitted
in Partial Fulfilment of the Requirements
for the Degree of
MASTER OF TECHNOLOGY

By
G. V. SRINIVASAN

to the

DEPARTMENT OF METALLURGICAL ENGINEERING
INDIAN INSTITUTE OF TECHNOLOGY KANPUR

DECEMBER, 1982

To

my grandfather

Late Shri T.V. Raja Rao

CERTIFICATE

This is to certify that the work on 'RECRYSTALLISATION AND TEXTURE STUDIES ON 0.26 WT. PCT. P-COPPER ALLOYS' has been carried out by G.V. SRINIVASAN under our supervision and it has not been submitted elsewhere for a degree.

(R. K. RAY)
Assistant Professor
Dept. of Metallurgical Engineering
Indian Institute of Technology
Kanpur.
(On leave to West Germany)

(K. P. Gupta)
Professor
Department of Metallurgical Engineering
Indian Institute of Technology
Kanpur.

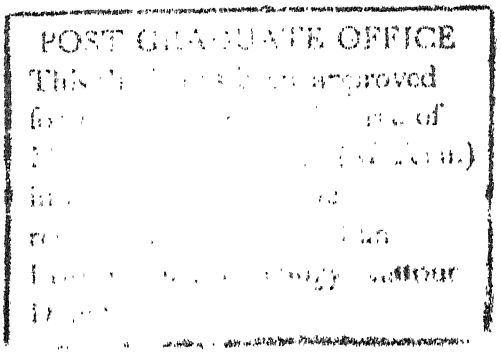

ACKNOWLEDGEMENTS

The author is deeply indebted to his thesis supervisors, Dr. R.K. Ray and Dr. K.P. Gupta, for their excellent guidance and interest they had on this work.

The invaluable assistance of Mr. E.V. Mathews, Research Scholar, throughout this work is greatfully acknowledged. The author wishes to thank Mr. S. Das, for his help on electron microscopic studies, Mr. G.S. Sharma, for his help on heat treatment of the alloys, Mr. K.P. Mukherjee, for his help on metallography, and Mr. M.L. Pandey, for his assistance on X-ray diffraction studies.

The author thanks Mr. R.N. Srivastava for neatly typing the manuscript and Mr. V.P. Gupta for his excellent drawings.

Finally, the author would like to express his sincere gratitude to all his friends, who made life at IIT Kanpur an enjoyable one.

- G.V. Srinivasan

TABLE OF CONTENTS

LIST OF TABLES

LIST OF FIGURES

ABSTRACT

Cold rolled specimens of pure copper and four different phosphorous containing copper alloys were examined in Transmission Electron Microscope (TEM). It was found that low phosphorous containing alloys had a clear cellular structure, while the higher phosphorous containing alloys did not show a clear cellular structure. Also, low phosphorous containing alloys showed cube oriented regions in their deformed matrix, while high phosphorous containing alloys did not show any cube oriented regions. Instead they showed presence of microtwins.

The alloy containing 0.26 wt. pct. phosphorous was chosen and annealed. The annealed samples were investigated in TEM. A partially annealed sample showed the presence of cube oriented regions, which had not recrystallised and had the characteristics of a deformed region. But in the same sample, many well recrystallised grains were seen, but their orientations were near to $\{110\}\langle 112\rangle$. It was also found that these well recrystallised grains had a similar orientation as that of the adjacent cold worked matrix.

Texture studies were done on the alloy for which the annealing studies were made. The room temperature cold rolled texture of 0.26 % P-Cu alloy resembled that of pure copper type texture, but texture was not quite sharp. When the same alloy was warm rolled at 100°C, a sharper copper type texture was produced. When rolled at 150°C the sharpness of copper type texture diminished. Annealing after room temperature rolling and warm rolling did not produce cube texture in the alloy. Their major annealing texture component was the same.

CHAPTER 1

INTRODUCTION

Recrystallisation involves nucleation and growth of strain free new grains in a deformed metal or alloy. Though considerable research has already been done on this phenomenon, the exact mechanisms governing this phenomenon have remained a subject of controversy. With the advent of Transmission Electron Microscopy and X-ray diffraction techniques, this phenomenon has been understood to some extent. But still the orientation aspects of nucleation, the mechanism by which a final preferred orientation prevails in a material are yet to be understood clearly. Attempts are now made to throw some light on this interesting phenomenon.

CHAPTER 2

LITERATURE REVIEW

As already been said, recrystallisation occurs when a deformed metal or alloy is heated to appropriate temperatures. Recrystallisation is preceded by recovery and grain orientation finally produced is strongly dependent on the deformed state. Hence before dealing with recrystallisation, it is imperative that one has a knowledge about the deformed state and its subsequent recovery stage. The literature review here deals with fcc metals and in particular with substitutional solid solutions, because for the present study, a fcc Cu-P substitutional alloy has been chosen.

2.1. The Deformed State

The deformed matrix can be defined as a damaged or heavily strained matrix full of defects like point defects, line defects, and planar defects[1], produced by means of plastic deformation, particle bombardment, quenching from high temperature etc. All these processes increase the defect density in the material.

2.1.1. Microstructure of Deformed Matrix

From the TEM observations made on polycrystalline fcc materials,[2,3] it is found out that the deformed matrix consists of a cellular structure. These cellular structures are in fact complex dislocation networks. It is also found that the cell density increases with increasing amount of deformation and

becomes more sharp at very high % of deformation. The interior of cells become free of dislocations while the cell walls are full of complex dislocation networks. Besides the dislocation network, some fcc metals show other effects of plastic deformation. For example, Hu et al.[4] have observed mechanical microtwins in α-brass. But observations of microtwins in pure copper, rolled at room temperature is rare. Microtwins are however, observed in pure copper rolled at -196°C. While clear subgrains could be found in pure copper, no such clear subgrains could be found in 70/30 brass.

2.1.2. The Stored Energy of a Deformed Matrix

A small amount (usually about 1 to 10%) of the energy spent in deforming a material remains 'stored' in the material causing an increase in the internal energy. This stored energy is the driving force for the recovery and recrystallisation processes. The magnitude of this stored energy is affected by the purity, method of deformation, temperature and grain size of the material.[1]

A plastically deformed material, due to its increased content of physical defects, is in a thermodynamically metastable state. So, when the matrix is slightly heated, it releases the stored energy. Haessner[5] classifies the steps through which the stored energy is released as follows:

(a) Reactions of point defects and point defect agglomorates - their annihilation.

(b) The annihilation of dislocations of opposite signs and the shrinking of dislocation loops.

(c) The rearrangement of dislocations to form energetically more favourable configurations (sub-boundaries).

(d) The absorption of point defects and dislocations by grain boundary migration.

(e) The reduction in the total grain boundary area.

Steps 'a' to 'c' are known as Recovery process and 'd' and 'e' are known as Recrystallisation. So these two processes depend on how the stored energy is released.

Impurities have a strong effect on the release of stored energy. DTA studies[6] reveal that the peaks are sharper for purer materials and for impure materials, a broad hump is observed over a range of temperatures. Also, it is seen that the release of energy takes place at higher temperatures for impure materials while for purer materials the energy release takes place at lower temperatures.

2.2. Recovery

J.G. Byrne[7] defines recovery as 'any modification of properties, during annealing, which occurs before the appearence of new strain free recrystallised grains, regardless of how refined the experimental technique used to detect the new grains'.

Mechanical and physical properties change very slightly during recovery. Electrical resistivity shows a rapid decrease from its coldworked value during the recovery anneal and a slower decrease as the annealing temperature is increased and recrystallisation starts. In the deformed state, the X-ray diffraction peak is broadened, because of heavy concentrations

of defects and increased strain in the lattice. On recovery anneal, the X-ray diffraction line tends to become sharp, because of reduction in strain energy and annihilation of the defects.

The kinetics of recovery process is found to follow the following relation

$$\text{Rate} = \frac{1}{t} = A \exp -(Q/RT)$$

where t is time, T is temperature, Q is activation energy for recovery, R is gas constant and A is a constant.

2.2.1. Mechanism of the Recovery Process

As recovery begins, the tangled dislocations in the cell walls rearrange themselves and some of the interior dislocations move to the cell walls. Some dislocations annihilate and the cell walls become more clearly defined and eventually form subgrains of about the same size as the initial cells.[7] Throughout this process the dislocation density continues to decrease in the cell interiors.

Based on dislocation rearrangement, the recovery process seem to operate by two mechanisms, namely, subgrain formation by coalescence and polygonisation.

In coalescence model,[8] dislocations move from the disappearing subgrain boundary into the connecting or interconnecting boundaries. This process requires dislocation climb along the dislocation subgrain boundary and a rotation of the subgrain itself, requiring movement of the atoms around the subgrain.

Polygonisation involves[9] climb and glide of edge dislocations of one sign to form a low angle tilt boundary, thus reducing the strain energy, which acts as a driving force for this process.

2.2.2. Influence of Impurities or Alloying on Recovery

Additions of impurity on alloying elements influences a retardation in the recovery process. Ray et al.[10] suggest that in Cu-P alloys, P influences a drag effect on dislocation migration, thus retarding the recovery processes compared to pure copper. The same views are supported by Lucke and Detert[11] and Hillert.[12] Even oxide inclusions retard the recovery processes.[13]

2.3. Recrystallisation

Recrystallisation involves nucleation and growth of strain free new grains. These new grains grow at the expense of the deformed matrix by high angle grain boundary migration. The driving force behind the recrystallisation process is the stored energy in the material produced during the plastic deformation.

2.3.1. Nucleation of Recrystallised Grains

Many theories of nucleation have been proposed since 1950. The classical theory of nucleation,[14] applied to homogeneous nucleation in liquid-solid transformation is as well applied here, with the assumption that the volume free energy is considered as the difference in strain energy per unit volume between the deformed state and the fully recrystallised state.

Though this theory could explain the order of magnitude of nucleation rate, incubation period for nucleation and preferential nucleation at the most severely strained regions, it somehow could not explain why the recrystallised nuclei that have high misorientations with deformed matrix are quite stable. This is contrary to the assumption that nuclei must have the same or near orientations with the adjacent deformed matrix. Hence the failure of this theory.

In another proposed mechanism nucleation occurs through subgrain growth.[14] In the initial stages two subgrains coalesce, which is really a recovery process, has been already explained. After the coalescence of two or more number of such subgrains, the angular misfit of regions surrounding the coalesced subgrains becomes greater. In order to minimise the strains around such a boundary, the boundary moves a little into the deformed matrix until an equilibrium stable position of the boundary is achieved. After subgrains coalesce by eliminating common subboundaries between them, the region thus formed has its radius greater than the critical radius for nucleation. This critical size coalesced region is not a recrystallised nuclei with a high misorientation with the adjacent deformed matrix.

Beck and Sperry[15] proposed the theory of 'Strain-Induced Boundary Migration', in which recrystallisation occurs by the movement of a portion of a boundary from a low energy grain having a coarser cell size, into a high energy grain having smaller cell size. The 'victim' grain is the one which is more severely work hardened, the stored energy of this grain providing the driving force for the entire process. In this model,

recrystallisation does not occur by nucleation and growth and hence the absence of incubation period.

Transition bands, regions of high local deformation and sharp lattice curvatures that result from inhomogeneous deformation are found in cold deformed metals. Sometimes nucleation occurs in the transition bands also. Dillamore's[16] analysis shows that

(a) For the nucleation of a recrystallised grain within the transition band, the local curvature of transition band should not be too high or too low but rather have an intermediate value.

(b) Nucleation will be favoured if there is a structure gradient of increasing dislocation density on either side of the centre of the orientation spread.

(c) The strains at which a transition band is such as to satisfy the above two conditions are determined by the way in which the crystal rotation is related to the orientation of the transition band.

2.3.2. Growth of Recrystallised Grains

Once a recrystallised nuclei has formed further growth takes place by grain boundary movement. The driving force for the grain boundary mobility are[17] (i) different residual strains in different grains leading to the continued growth of those less strained grains, and (ii) the surface energy of the grain boundaries. The rate of boundary migration is controlled by the rate of atom transfer across grain boundaries and proportional to the curvature of the cells or inversely proportional

to the radius of curvature.

The growth depends on the orientation of the growing grain with the adjacent grain. Generally a high angle grain boundary migrates fast because of easy transportation of atoms across the boundary. But there are some special boundaries, called Kronberg boundaries,[18] or coincidence boundaries. This coincidence boundary consists of an array of points common to the lattices of both the grains, and according to Kronberg the presence of high density of coincidence atoms can make the boundaries highly mobile. Also it is said that the highest migration rate in fcc metals has been obtained when the growing grain is crystallographically related to the matrix by a 30-40° rotation about a common $\langle 111 \rangle$ axis.[18]

Impurities or alloying elements very much affect the grain boundary mobility. Cahn[19] says that when substantial amounts of solute are present, they exert such powerful control over boundary migration, that the orientation differences lose their influence. Lucke & Detert,[11] and Ray & Hutchinson[20] have shown that alloying elements influences a drag effect on the mobility of high angle grain boundaries.

2.4. Texture

When a polycrystalline material is plastically deformed by rolling, the lattice orientations in individual grains change and a crystallographic direction uvw tend to align in the direction of deformation given and a crystallographic plane hkl becomes parallel to the rolling plane. This preferred grain orientation is called "texture" and is expressed by

$\{hkl\}\langle uvw\rangle$. This orientation is very characteristic of the material itself and also depends on the variables controlling the deformation process. When the same material is annealed, or recrystallised, the grain orientations often change to new ones resulting in new texture. This texture transition again depends on many variable parameters.

2.4.1. Description of Textures

Since it is very difficult to state the orientation of each and every grain, X-ray diffraction method is used to yield an overall picture of grain orientation. The pole figures are obtained using the transmission and reflection methods.[21] The pole densities in a pole figure are compared with standard pole locations on a plane of projection which is parallel to the rolling plane and is normally expressed by indicating deviations of pole location in a pole figure from the ideal orientation.

Bunge and Heassner[22] have described texture by means of orientation distribution function (ODF). These ODF can be derived from selected area electron diffraction patterns as well as from the X-ray diffraction data. But the computation of this ODF is very complex and hence the conventional pole figures are widely used because of their simplicity.

2.4.2. Deformation Textures of FCC Polycrystals

The nature of the deformation texture depends[23] on crystal structure, impurities and alloying element content, deformation characteristics of the metal or alloy temperature of deformation, the deformation process itself, initial texture if any, previous thermal or mechanical treatment etc.

Two types of deformation textures are normally observed in fcc materials.[4] One is called the 'Pure Metal' type (copper type) and the other is called as 'Alloy type' (α-brass type). Most of the fcc metals, except silver, show pure metal type rolling texture, while silver and alloys show alloy type rolling texture.

The ideal orientation of the copper type texture is designated as $\{123\}\ \langle 41\bar{2}\rangle$, while some others[24] designate the pure metal orientation as a combination of $\{110\}\ \langle 1\bar{1}2\rangle$ and $\{112\}\ \langle 11\bar{1}\rangle$ orientations. The ideal orientation of the α-brass type texture is designated as $\{110\}\ \langle 1\bar{1}2\rangle$. The rolling textures for copper type and brass type are shown in Figure 2.1.

2.4.2.1. Texture Transition in Deformed State

Smallman[25] has observed that addition of solute elements to pure metal transforms the pure metal type rolling texture to an alloy type rolling texture. Addition of 10% Zn to pure Cu, changes the pure metal copper type texture into a brass type texture. It is implied here that the greater is the misfit of solute with solvent, lesser is the amount of solute required to transform the texture to brass type rolling texture.

Hu et al.[4] showed that the decrease in temperature of deformation the pure metal type texture changes into brass type. Copper rolled at -196°C changes to brass type texture. However, the temperature dependence of texture transition is very sensitive to impurity contents. Smallman[26] showed that very high purity copper (99.999%) rolled at -196°C did not

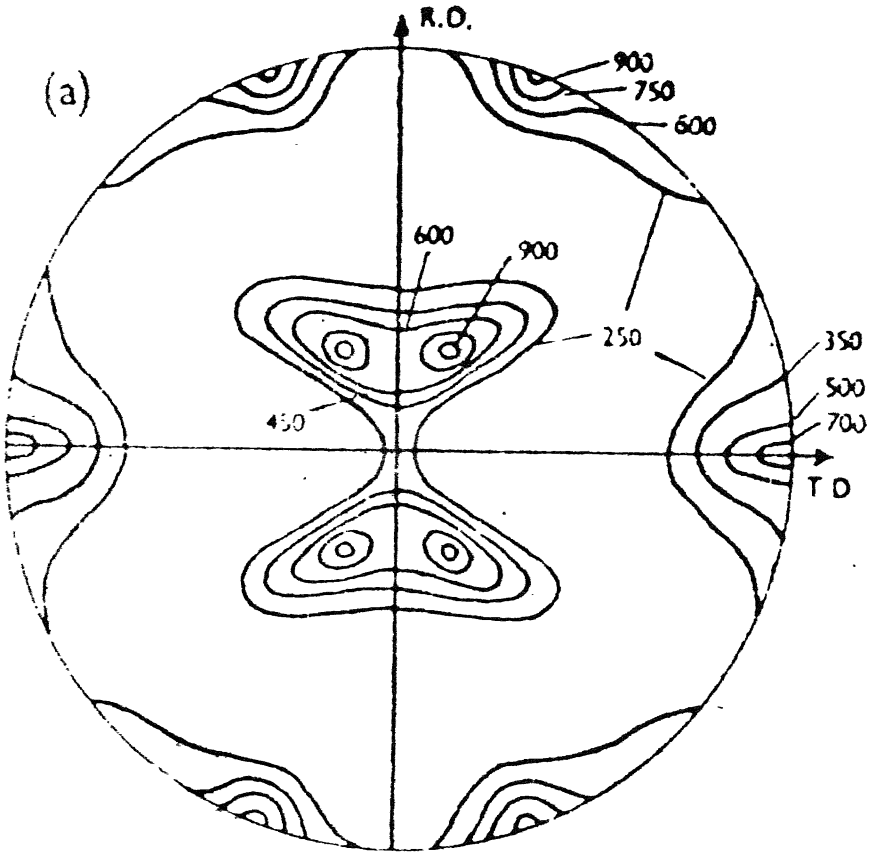

Fig. 2.1(a). (111) Texture pole figure of room temperature rolled pure copper.

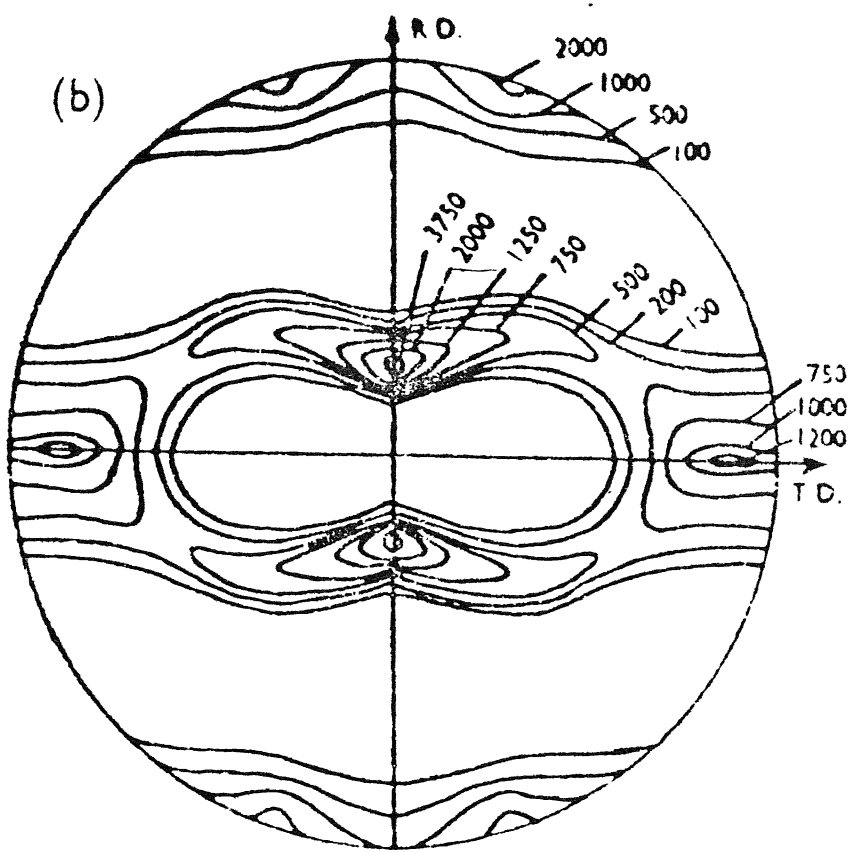

Fig. 2.1(b). (111) Texture pole figure of room temperature rolled α-brass.

produce any change in pure metal type texture. But the 99.99% pure Cu, showed some transition when rolled at -196°C.

Rolling at elevated temperatures is also found to produce a sharp pure metal type texture. Smallman[25] reported that Cu - 5% Zn α-brass when rolled at -183°C produced the usual brass type texture, but when rolled at 200°C produced a sharp copper type rolling texture. Hu et al.[4] attributes the texture transition to change in stacking fault energy.

Wierzbanowski[27] has summarised the mechanisms that are responsible for the texture transition, as follows:

(a) Addition of the $\{111\}\ \langle 11\bar{2}\rangle$ slip system to the normal $\{111\}\ \langle 1\bar{1}0\rangle$ slip causes the texture to change from the pure metal type to alloy type.

(b) Mechanical twinning on the $\{111\}\ \langle 11\bar{2}\rangle$ system changes pure metal to alloy type texture.

(c) Activation of additional slip systems, i.e., $\{100\}\ \langle 110\rangle$ and $\{110\}\ \langle 110\rangle$ to normal $\{111\}\ \langle 110\rangle$ causes the alloy type to pure metal type texture.

(d) Cross-slip in significant amount induces the alloy to pure metal type texture transition.

2.4.3. Recrystallisation Texture

2.4.3.1. Recrystallisation Textures of Polycrystalline FCC Materials

It is known that till 50% reduction in thickness, the annealing texture is almost random.[28] Many fcc pure metals like copper, after cold rolling to high amount of deformation gives cube texture on annealing. The cube texture is very sharp if

the deformation is between 95% and 99%, and is often accompanied by its twin component $\{122\}\ \langle 212\rangle$. But cross rolled copper does not recrystallise in cube texture.[28]

On adding solute elements to pure copper, the sharpness of cube texture decreases. Merline and Beck[29] noticed that 10% of Zinc addition to pure copper, completely suppressed the cube component in the recrystallisation texture. The (111) pole figures for the 3%, 6%, 10%, and 30% Zn brass after recrystallisation are given in Figures 2.2 and 2.3. Six main components are seen in those pole figures and they are given in Table 2.1.

Table 2.1. Recrystallisation Texture Components of -brass

Component	3% Zn	6% Zn	10% Zn
A	(368) [$42\bar{3}$]	(368) [$42\bar{3}$]	(256) [$94\bar{6}$]
B	(214) [$52\bar{3}$]	(427) [$42\bar{3}$]	(438) [$63\bar{4}$]
C	(001) [100]	(001) [100]	(001) [100]
F	(112) [$20\bar{1}$]	(112) [$20\bar{1}$]	(112) [$20\bar{1}$]
M	(047) [100]	(037) [100]	(038) [100]
S	(125) [$55\bar{3}$]	(125) [$33\bar{2}$]	(338) [$44\bar{3}$]

Pure copper (99.98%) rolled at -196°C had the Cu - 6% Zn rolling texture. But the annealing texture of low temperature rolled copper is different from the annealing texture of Cu - 6% Zn brass.

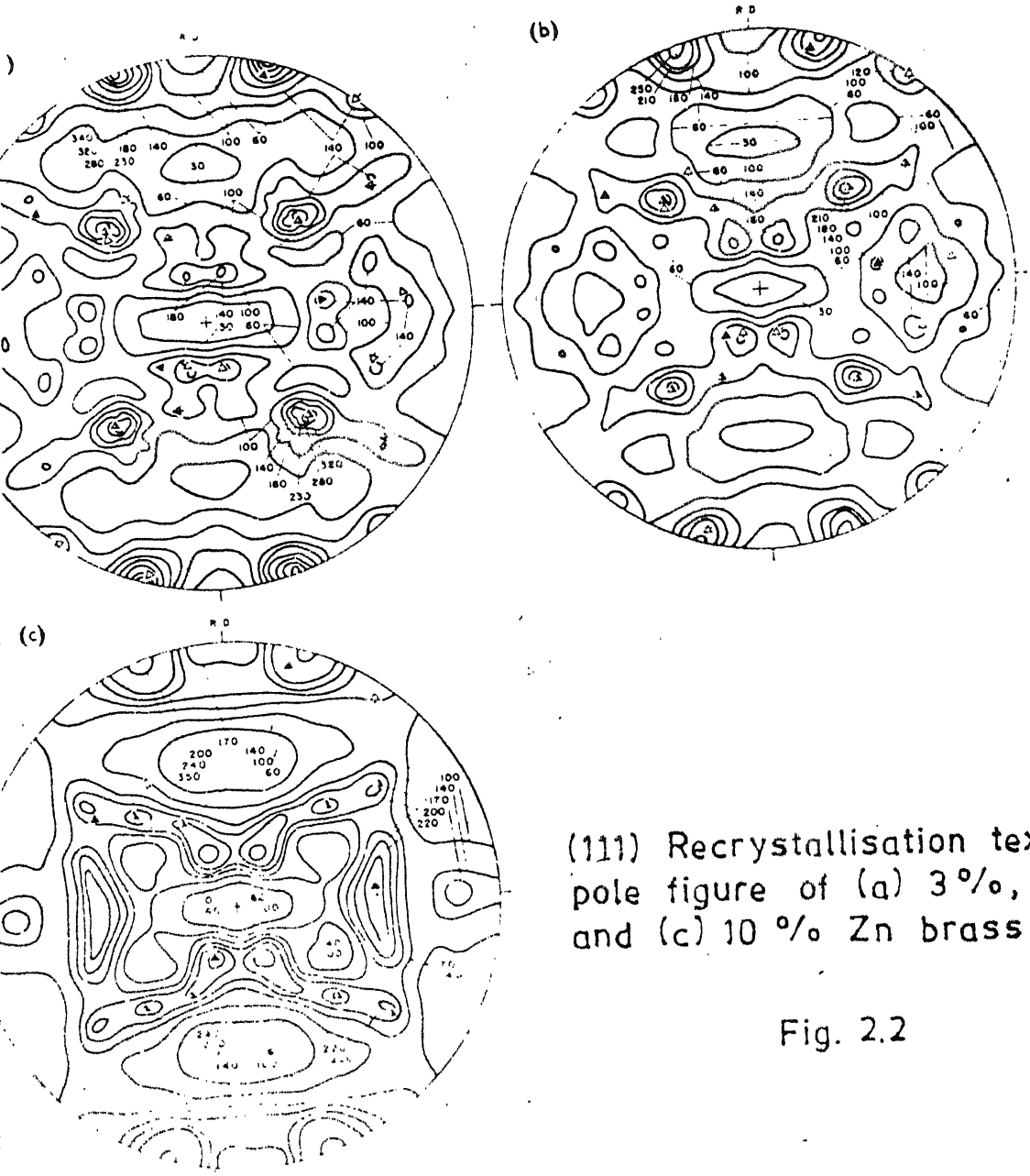

(111) Recrystallisation texture pole figure of (a) 3 %, (b) 6 % and (c) 10 % Zn brass.

Fig. 2.2

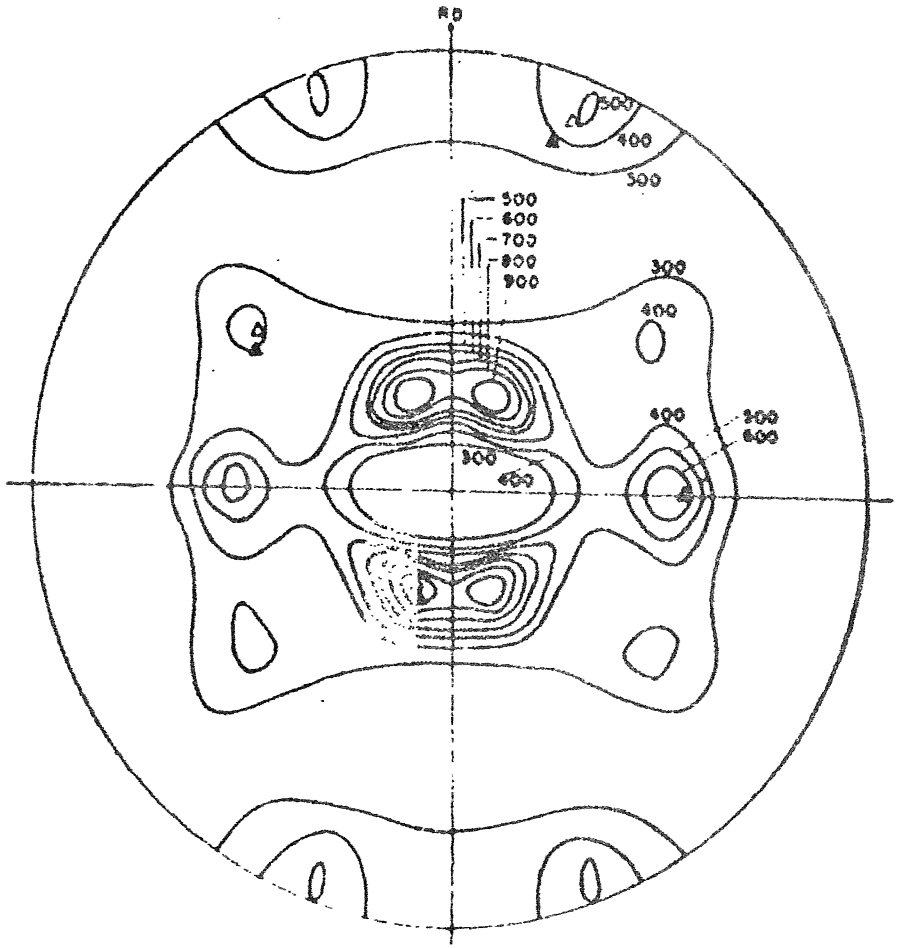

Fig. 2.3 (111) Recrystallisation texture pole figure of 70/30 brass.

Most of the recrystallisation orientation components in brass have a 30-40° ⟨111⟩ rotational relationship with the copper type texture. Most of the substitutional solid solution of fcc metals show similar annealing textures as that of brass. But Richman and Liu[30] have reported that the annealing textures of Cu-P, Cu-As, and Cu-Sb solid solution are different from α-brass. For example, a (111) recrystallisation pole figure of Cu - 0.52 wt. % P alloy is as shown in Figure 2.4.

2.4.3.2. Theories of Formation of Recrystallisation Textures

The final orientations present in the fully recrystallised material require both the presence of nuclei in these orientations and the ability of these recrystallised grains to grow during the annealing process. In search for the origin of recrystallisation textures, one of the principal questions to be answered is whether the orientations absent from the recrystallisation texture are suppressed because of the unavailibility of nuclei in these orientations or because of the inability of such nuclei to grow to an appreciable volume in competition with nuclei of other orientations. These form the basis for the two theories that have been put forward to explain the development of recrystallisation textures.

In the oriented nucleation theory[31], the nucleation process is supposed to be of primary importance in determining the range of available nuclei which can contribute to the recrystallisation texture. In the oriented growth theory, proposed by Barrett[28], the recrystallisation texture is supposed to be the result of growth selection due to orientation dependence

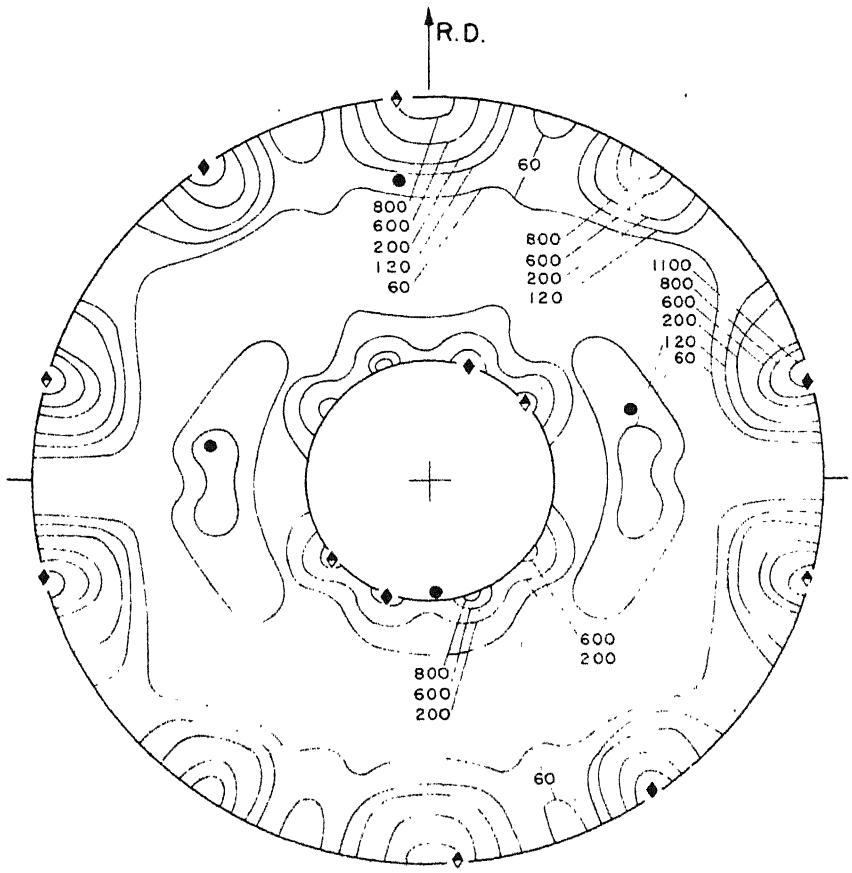

Fig. 2.4 —{111} —Pole figure of a Cu–1.03 at. pct P alloy rolled 99.3 pct and annealed 1 hr at 400°C.
♦ — {110} <112> + 14° ◈ — {110} <112> —16°
● — {227} <774> — I

of the rate of grain boundary migration.

Many workers[32,33] since then have supported one of the theories and opposed the other. Even in the latest conference on 'Texture of Materials' held at Aachen, West Germany 1978, many authors[34-37] have expressed these opposing views. Naka et al.[37] and Ray et al.[38], however, have observed that both oriented nucleation and oriented growth play important role in the recrystallisation texture development.

CHAPTER 3

STATEMENT OF THE PROBLEM

It is clear from the literature that the phenomenon of Recrystallisation requires further investigation to understand texture development in metals and alloys. Research on some binary alloys will be helpful as it will also show the effect of alloying elements on recrystallisation and texture development processes. Since the interpretation of mechanisms may become complicated if a second phase comes into picture, the choices of alloy should be one having a single phase, i.e., a solid solution alloy.

Much work has already been done on fcc metals like pure copper, and substitutional alloys like α-brass. Unlike copper, and α-brass, Cu-P, Cu-As, Cu-Sb, all with group VB alloying elements, show a different recrystallisation behaviour as far as texture development is concerned.[30,31] Hence in this work an attempt has been made to study the effect of phosphorous on the recrystallisation and texture development process in Cu-P alloys. Since only very little work has been done on the effect of warm rolling on the recrystallisation texture development, in this investigation a preliminary study on this aspect has been planned.

The present study envisages study of deformed state and recrystallisation stages of Cu-P alloys through transmission electron microscopy. Most of the study is expected to be

concentrated on a Cu-P alloy containing 0.26 wt. % P (alloy C). Recovery and Recrystallisation kinetics is proposed to be studied through X-ray line broadening[10] and electrical resistivity techniques[7] and through quantitative metallographic techniques respectively. Finally the texture studies of rolled and annealed materials are expected to be determined quantitatively through X-ray diffraction techniques.

CHAPTER 4

EXPERIMENTAL PROCEDURE

4.1. Material and Initial Treatment

A pure copper (99.998% purity) and four copper-phosphorous alloys of compositions; as shown in Table 4.1 were chosen for the present study.

Table 4.1. Alloy Compositions Considered.

Alloy	wt. % of P
A	0.00
B	0.16
C	0.26
D	0.76
E	1.44

The alloys and pure copper were supplied by Thonson Matthey & Co., U.K.

The ingots were about 6" long with a rectangular cross-section of approximately 0.32 square inch area. All the five ingots were homogenised at 700°C, for 24 hours, embedded in graphite powder. Then all the five ingots were rolled down to 0.1" thickness in second step; each step was followed by annealing of the sample at high temperature for some time. Then

the alloy A was annealed at 600°C for 5 hours and the alloys B to E, were annealed at 700°C for 5 hours. The grain size were found to be similar in all the samples, ($\sim$ 0.05 mm). Texture determined at this stage showed complete randomness in grain orientation in the sheet samples.

4.2. Cold Rolling

The pure copper and the four copper-phosphorous alloys were rolled down from an initial thickness of 0.1" to 0.005" giving 95% reduction in thickness. The reduction per pass was not more than 10% and the samples were reversed end to end for every pass. The sample was immersed in cold water from time to time to remove the heat produced during the rolling.

4.3. Warm Rolling

The alloy 'C' was warm rolled to 95% reduction in thickness at 100°C and 150°C. The furnace was kept at 50°-60°C higher than the rolling temperature. The temperature of the sample was measured with a thermocouple, its hot end touching the surface of the sample and a multi range APLAB microvoltmeter was used to measure the temperature. The specimen was allowed 15 to 20 minutes in the furnaces to attain uniform temperature and then brought to the rolls. When the temperature of the sample dropped to the rolling temperature, it was immediately pushed between the running rolls and then the rolled material was again put back into the furnace. It was ensured that the reduction per pass was not more than 10%.

4.4. Annealing

The rolled strips were cut into 1" x 1" size. The annealing of the sample was done in a salt bath containing a mixture of sodium nitrate and potassium nitrate, each in equal amounts. The thermocouple properly sheethed in a closed end stainless steel tube was put in the salt bath and the temperature of the salt bath was controlled by a Leeds-Northrup 6260 on-off temperature controller. Another sheathed thermocouple was also put in the salt bath to measure accurately the actual temperature of the salt bath. A Leeds-Northrup potentiometer was used for this purpose. The bath temperature was maintained to within $\pm$ 3°C for any chosen annealing temperature. Annealing was carried out at three different temperatures, viz., 275°C, 300°C, and 325°C,for different lengths of time,,varying from 1 minute to 50 hours. All the samples were water quenched after completion of each heat treatment. The surface of the samples were cleaned by a 2% nitric acid solution and dried. These annealed samples were later used for electron microscopic investigation, kinetics and texture studies.

4.5. Electron Microscopy

Samples of size 2 mm x 15 mm were cut from the 1" x 1" sample along the rolling plane. Then they were chemically thinned by a 50% nitric acid solution, until the sample floated on the solution. Then the sample was cleaned and electropolished. The electrolyte was 33% nitric acid and 67% methanol solution, surrounded by ice water bath. Some liquid nitrogen was poured on the bath from time to time to have the temperature of the

electrolytic bath around 0°C. Stainless steel was used as cathode and a voltage of 6-8 V was applied for electro polishing. The edge of the thinned sample was cut by a scalpel and used as electron microscopic specimen. In cutting out the specimen, care was taken to have the cut edge either along the transverse direction (TD) or along the rolling direction (RD). For each specimen the cut edge orientation was noted down. All the electron microscopic studies were carried out in a Phillips EM 301 Transmission Electron Microscope, with an operating voltage of 100 KV. The photographs were taken on a 35 mm film and processed. Cut edge pictures were also taken to determine the relative orientation of a crystal grain relative to the RD or TD.

4.6. DTA Studies

Differential Thermal Analysis was performed on alloys A and C only. In each case, a thin strip of the same alloy was fixed in a stainless steel tube of wall thickness 0.01" and dia 1/8" to act as a specimen holder. Samples of each size 1.5 mm x 1.5 mm were cut and stacked closely inside this specimen holder. The stainless steel tube was long enough to insert the DTA thermocouple into it, so as to be in good contact with the specimen strip, as shown in Figure 4.1.

In this technique the emf produced by the thermocouple touching the alloy sample was set in continuous opposition to the emf produced by a thermocouple attached to a standard reference sample (pure copper), and the difference emf of the balanced pair of the thermocouple was amplified by a Leeds and

Northrup microvolt amplifier and recorded on a strip chart recorder. Temperature was measured as a function of time using a Leeds-Northrup potentiometer. The sample and the reference sample were heated in a close proximity to each other with a heating rate of 2° per minute, controlled manually. A standard sample as standard sample DTA run was also made to determine the base line characteristics of DTA apparatus. The experiment was done in Argon atmosphere to avoid oxidation.

4.7. Recovery Studies

Two sorts of experiments were carried out to study the kinetics of recovery of the alloy C. One is through peak broadening method using the X-ray diffraction technique and the other is through electrical resistivity measurements.

4.7.1. X-ray Diffraction Technique

A sample of size 8 mm x 25 mm was cut from 95% cold rolled sheets. The surface of the sample was polished by a 4/0 emery paper and then chemically cleaned by a 4% nitric acid solution. Then the specimen was positioned in a diffractometer and diffraction traces of (111), (200) and (220) peaks were traced. Higher chart speed was used to get a broad peak for easy and more accurate measurements of peak breadth. Then the same sample was annealed in a salt bath furnace, cleaned as before and the diffraction peaks were traced. All the annealings for different lengths of time at a specified temperature were done on the same sample to ensure that the peak intensity and the breadth did not depend on the characteristics of the

specimen. Annealing time was taken as cummulative. First the experiments were carried out in General Electric XRD VI X-ray diffractometer, and later more sophisticated Rich-Seifert X-ray diffractometer was used in both automatic point counting as well as peak trace modes. For processing point count data, a DEC-10 computer was employed to trace an enlarged peak consisting of nearly 120 points per peak. The X-ray line broadening techniques were tried with specimens annealed at 275, 300, and 325°C.

4.7.2. Resistivity Measurements

To study the kinetics of recovery dynamically, resistivity measurement method was tried. In this method, the voltage drop across the specimen, was recorded continuously on a strip chart recorder as the specimen was going through recovery annealing process. A narrow strip, 2 mm wide and 60 mm long, was cut (the shape shown in Figure 4.2) from the cold rolled sheet and copper wires were spot welded. A four probe measuring technique was applied. A precisely controlled 20 mA direct current was passed through the specimen and voltage drop across 50 mm length of the specimen was continuously monitored, after amplification, on a strip chart recorder. The sample was immersed in a controlled temperature silicone oil bath kept at a desired temperature. As soon as the sample was immersed in the oil bath, the recorder was switched on, to record emf change with time. The specimen annealing was carried out until a no more drop in emf could be detected.

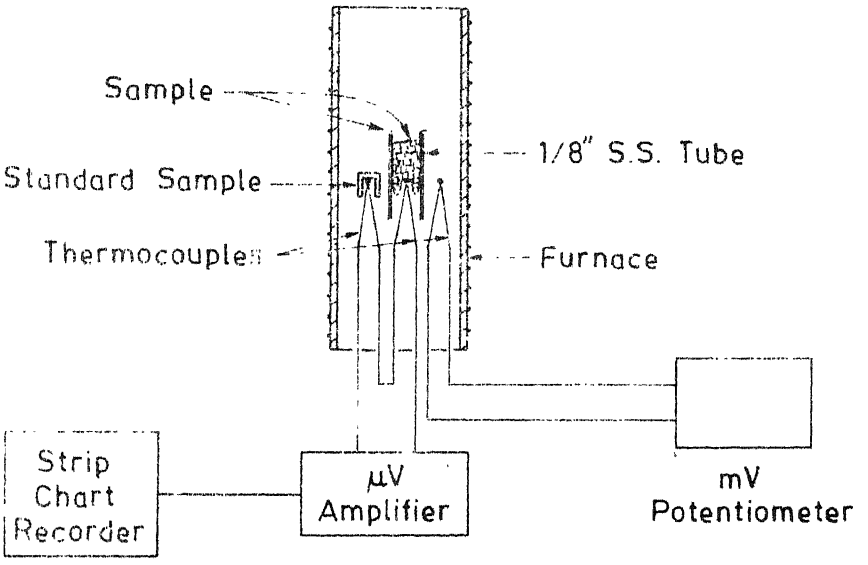

Fig. 4.1. Schematic for the DTA setup.

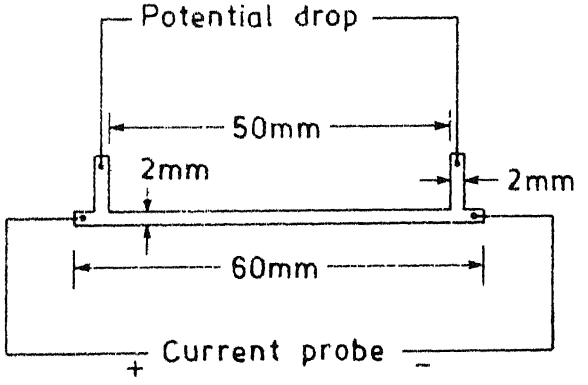

Fig. 4.2. Resistivity sample.

4.8. Metallographic Study of Recrystallisation Kinetics

Kinetics of recrystallisation experiments were carried out by optical microscopy method. Samples of size 3 mm x 15 mm were cut from all the cold rolled, annealed materials and mounted in transparent plastic. First all the mounted samples were mechanically polished and then electropolished. The electrolyte found suitable for its purpose was a 40% phosphoric acid solution. Voltage of about 4-5 V was supplied from a constant dc power supply, a stainless steel strip was used as a cathode. Electrical contact with the sample (anode) was made by the forceps which held the specimen in the electrolyte. After electropolishing, the sample was washed in running water and dried.

Electro etching was done in the same electrolyte, but the voltage was reduced to 1-2 V. The etched surface was observed in a Carl-Zeiss No. 2 optical microscope and several regions were photographed and finally enlarged prints were prepared. A square grid with 25 points was placed on the micro-photograph and the fraction recrystallised was determined by the point-counting method. This was repeated in all the samples, that were annealed at different temperatures, to different timings.

4.9. Texture Determination

Texture of the cold rolled, warm rolled and annealed samples were measured by the X-ray diffraction method. Texture studies were made on alloy 'C' only. Reflection method was employed. The samples of 20 mm x 20 mm size were well polished

and cleaned by 4% nitric acid. All the samples were of the same thickness. They were mounted on a Phillips X-ray texture goniometer, which was set to give the (111) reflection. Cu_{K_α} X-radiations was used and a voltage of 40 KV and a current of 30 mA was given. The reflected rays were detected by a scintillation counter, and the peaks were recorded on a strip-chart recorder. The intensities of the textured samples were compared with a random well annealed copper powder sample having no texture, and the relative intensity ($I_{sample}/I_{random\ sample}$) was plotted on a spiral chart of 5° pitch. Plotted intensities were then used to draw intensity contour lines to depict pole densities in (111) pole figure. Standard pole projections were used to determine the approximate texture components.

CHAPTER 5

RESULTS

5.1. Studies on Deformed State

5.1.1. Deformation Microstructures

Electron microscopic studies on all the four Cu-P alloys and pure copper were made after they had been cold rolled to 95% reduction in thickness. Several specimens were studied but only few representative micrographs and diffraction patterns are shown in Figure 5.1 to Figure 5.10 and Figure 5.14. It can be seen from Figures 5.1, 5.2 and 5.3 (for alloys A, B and C) that the specimens A, B and C, all have a clear cellular structure. On the other hand the alloys D and E (Figures 5.4 and 5.5) do not show clear cellular structure in the 95% deformed state. Possibly the cell sizes are too small in these alloys to be seen clearly. But twinning was found more frequently in alloys D and E (Figures 5.6 and 5.7), and it was found that alloy E had higher frequency of occurrence of twins. This may be expected, as with increase in alloying element content, the stacking fault energy decreases rapidly.

Present studies show that for pure copper (specimen A) and low phosphorous containing alloys B and C, the deformed state had regions with cube orientation, as can be seen from Figures 5.8(a), 5.8(b), 5.9(a), 5.9(b), 5.10(a), and 5.10(b). On the other hand in higher phosphorous containing alloys, D and E, no cube oriented regions could be found.

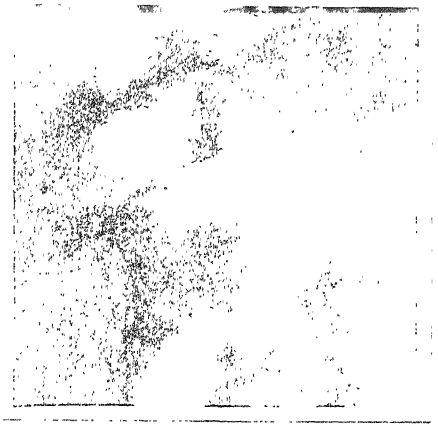

Figure 5.1. A typical cold worked area of pure copper, sample A. Mag. 20,000.

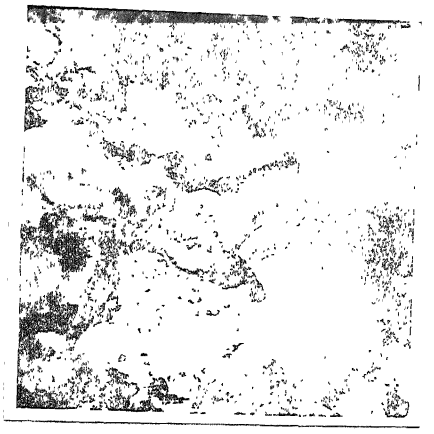

Figure 5.2. A typical cold worked area of alloy B. Mag. 20,000.

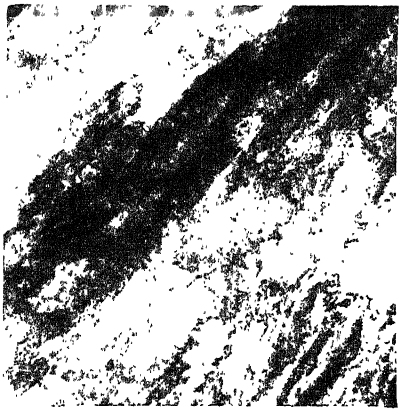

Figure 5.3. A typical cold worked area of alloy C. Mag. 20,000.

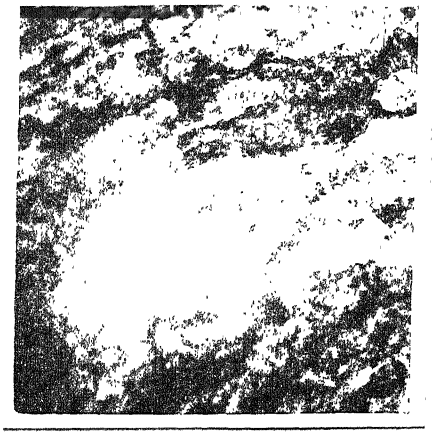

Figure 5.4. A typical cold worked area of alloy D. Mag. 20,000.

Figure 5.5. A typical cold worked area of alloy E. Mag. 20,000.

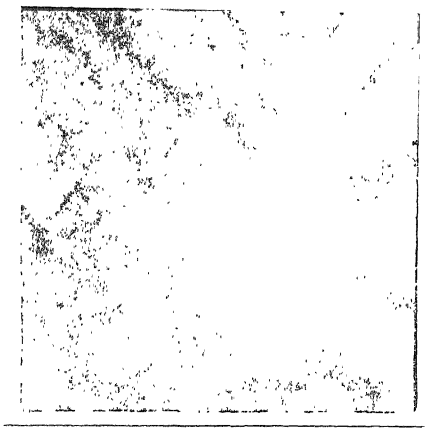

Figure 5.6. A cold worked area of alloy D containing twins. Mag. 34,000.

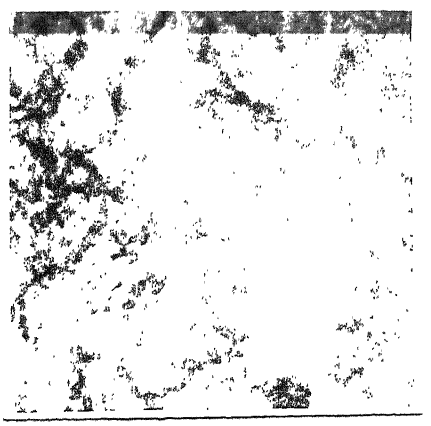

Figure 5.7. A cold worked area of alloy E containing many microtwins. Mag. 20,000.

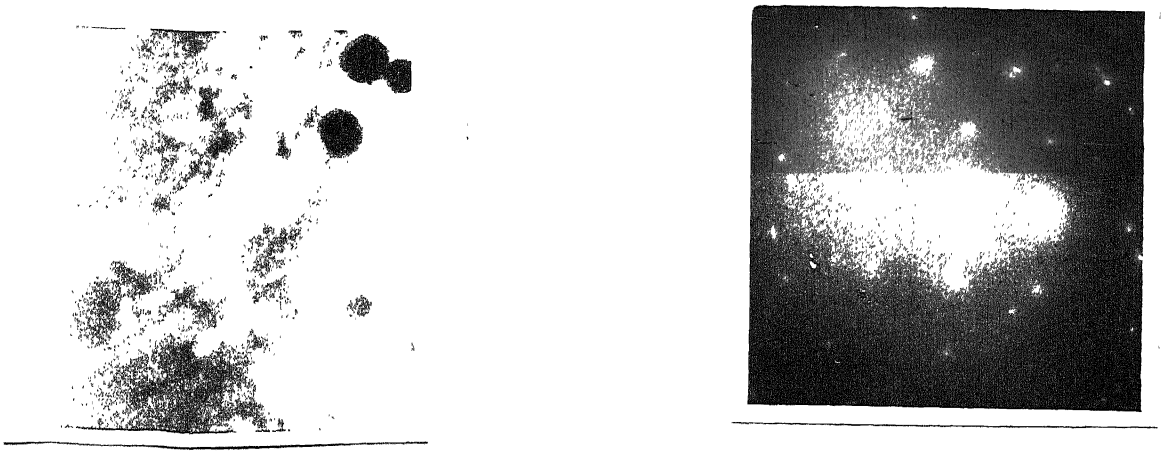

(a) Mag. 12,600. (b)

Figure 5.8. Presence of a cube oriented region in cold worked matrix of pure copper.

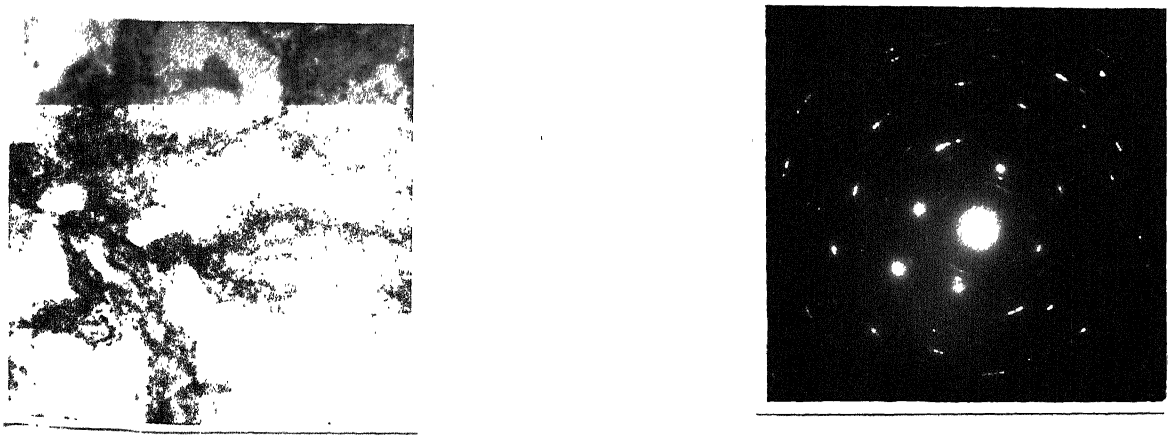

(a) Mag. 44,000. (b)

Figure 5.9. Presence of a cube oriented region in cold worked matrix of alloy B.

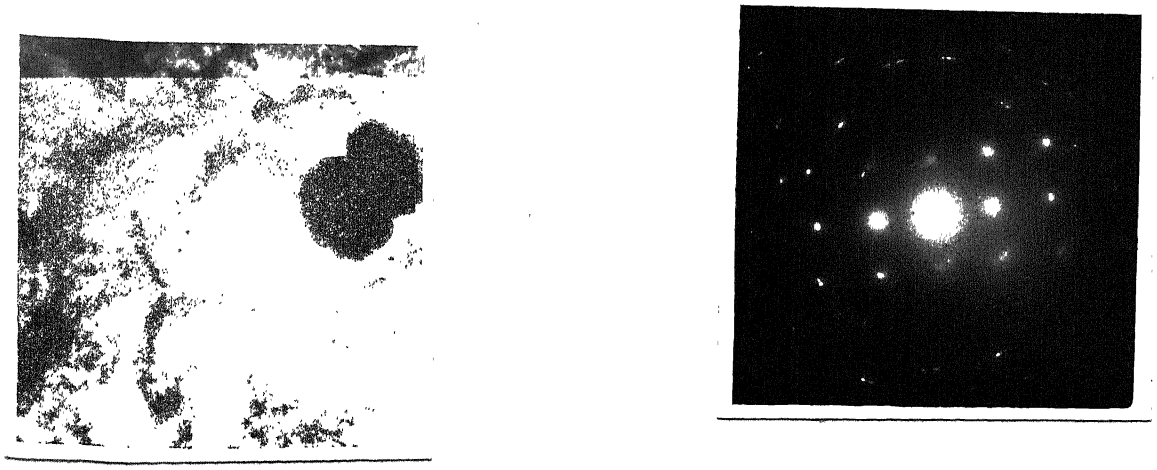

(a) Mag. 20,000. (b)

5.1.2. Deformation Textures

Since deformation texture of alloys A and B had been studied earlier[10], in this investigation deformation texture was studied only for alloy C. Texture studies with 95% cold rolled alloy C revealed that its deformation texture (Figure 5.11) resembles somewhat with the pure metal (copper type) texture. But it did not show sharp copper type texture (commpare with Figure 2.1). If $\{123\}\ \langle 41\bar{2}\rangle$ is considered as the ideal orientation of the pure metal type texture, then cold rolled alloy C shows its main texture component is nearly 20° away from the ideal $\{123\}\ \langle 41\bar{2}\rangle$ pole location along the rolling direction.

The same alloy on 95% reduction in thickness by warm rolling at 100°C showed a more sharp copper type texture (Figure 5.12). The main texture component in this case coincides with that of the ideal pure copper type orientation $\{123\}\ \langle 41\bar{2}\rangle$. It can be also seen that the intensity of the main texture component in the warm rolled at 100°C alloy shows a higher intensity level compared to the same alloy rolled at room temperature. The sharp copper type texture is possibly due to cross slip.[27]

But when the same alloy is warm rolled at 150°C, the alloy showed again a weak pure metal type texture. Figure 5.13 shows that the main texture component is 3-5° off from the ideal orientation $\{123\}\ \langle 41\bar{2}\rangle$ along the rolling direction. Also the main texture component intensity level has decreased compared to the one rolled at 100°C. Moreover the alloys rolled at room temperature and rolled at 150°C also showed a minor texture component, possibly $\{225\}\ \langle 734\rangle$.

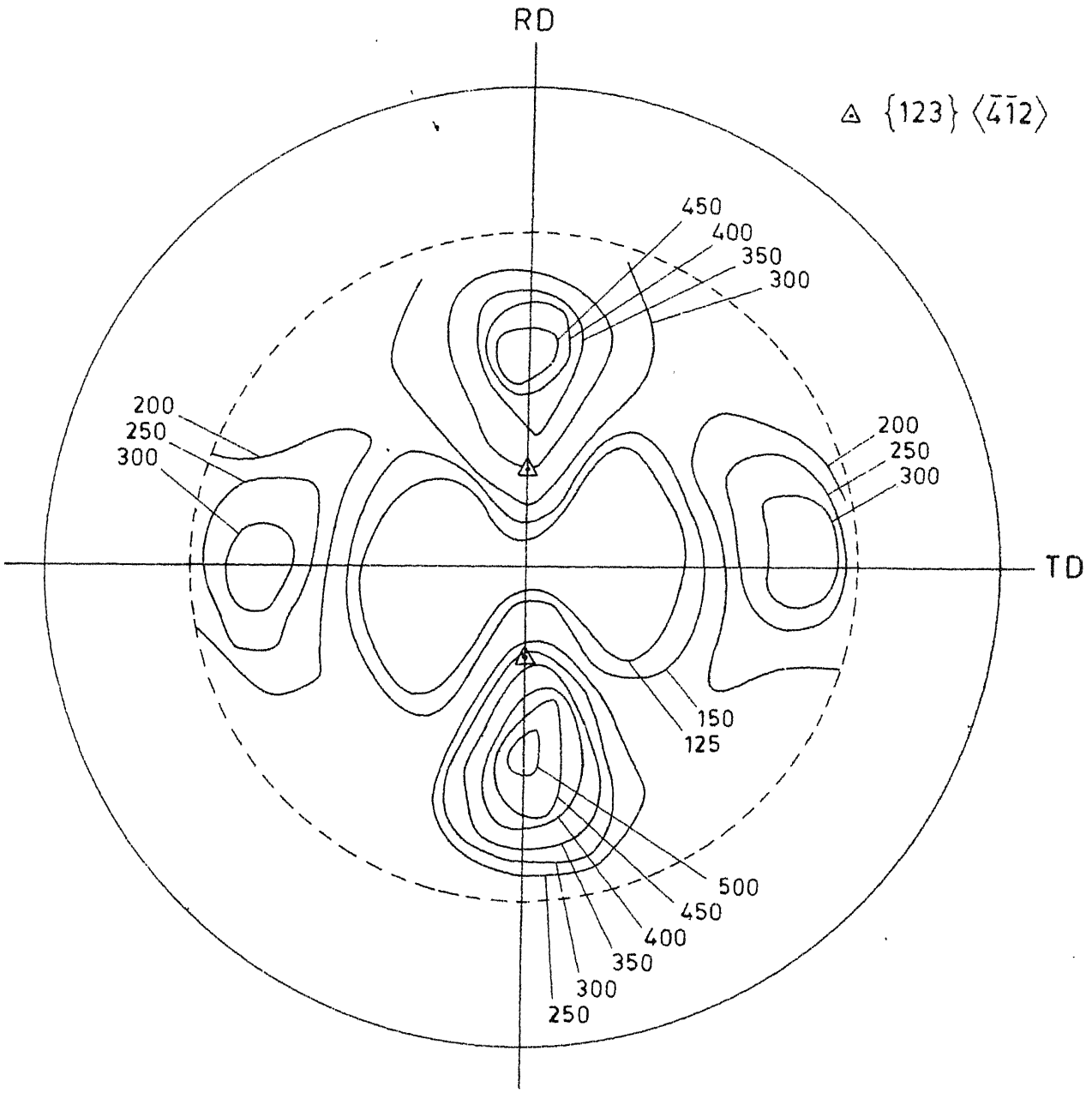

Fig. 5.11. (111) Pole figure of a room temperature coldrolled alloy C.

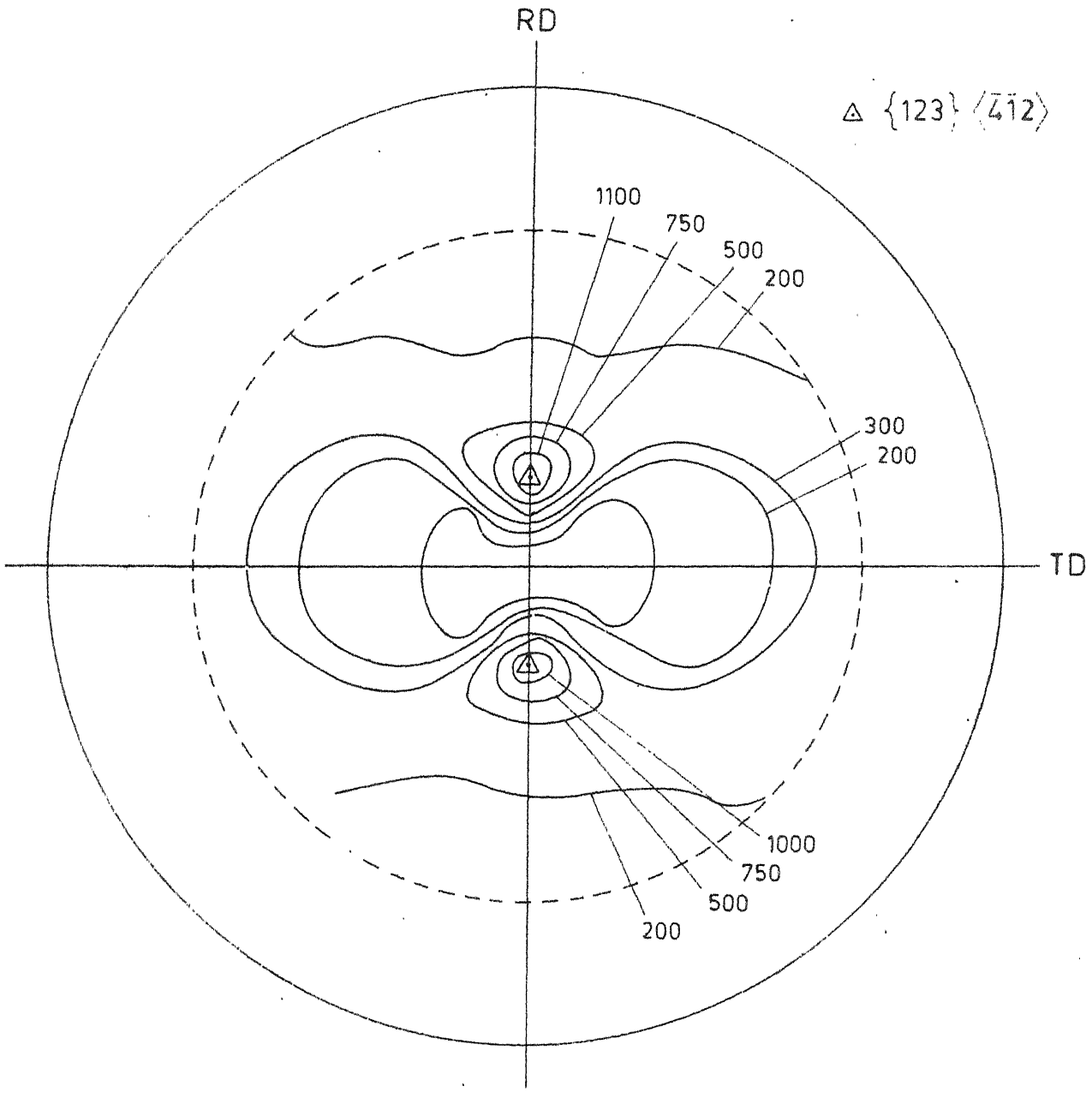

Fig. 5.12. (111) Pole figure of alloy C warm rolled at 100° C.

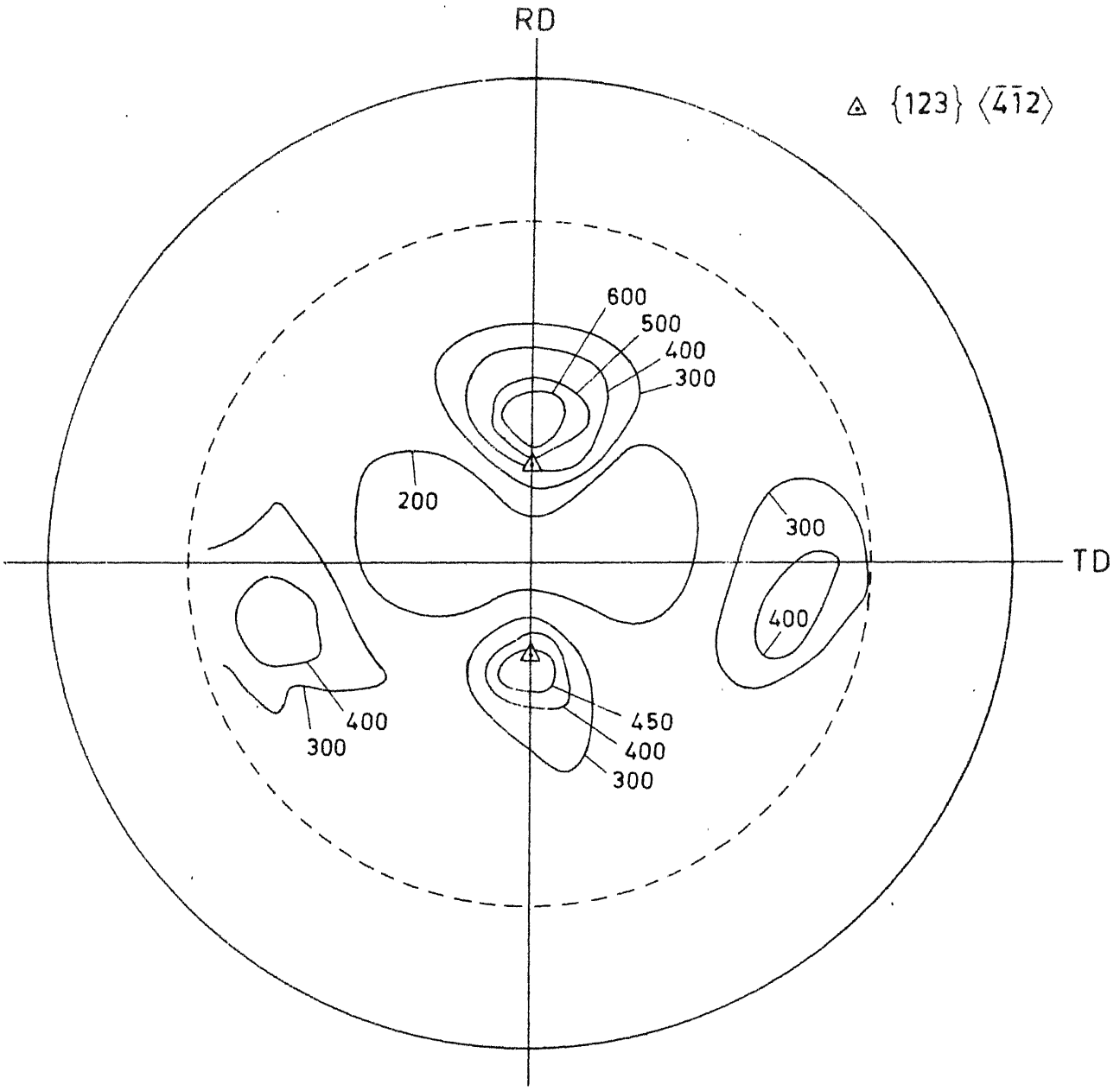

Fig. 5.13. (111) Pole figure of alloy C warm rolled at 150° C.

Though for simplicity an ideal orientation of $\{123\}\langle 412\rangle$ is used to describe the rolling texture of a pure metal, the actual intensity distribution in a pole figure around this ideal orientation is due to many crystal orientations which are somewhat different. For example, the intensity distribution around the ideal $\{123\}\langle 412\rangle$ covers also the following texture components: (110) $[1\bar{1}2]$, (110) $[001]$, (110) $[1\bar{1}0]$, (112) $[11\bar{1}]$ etc. Some of these orientations have been actually seen in the TEM study of the cold rolled alloy C specimens (Figures 5.14(a), 5.14(b) and 5.14(c)).

5.2. Studies on Recrystallisation

5.2.1. TEM Investigations of Recrystallisation

Annealed samples were examined in a Phillips301 transmission electron microscope. It can be seen from Figures 5.15(a), 5.15(b), that cube oriented regions are still present, but these regions do not show fully recrystallised structure. On the other hand, in the same sample, these are well recrystallised grains (Figure 5.16(a)), and they do not have cube orientation (Figures 5.16(b)). The Figures 5.16(a,b,c) show that the recrystallised grain has a similar grain orientation as the adjacent cold worked matrix. It is found that most of the recrystallised grains have $\{110\}\langle 1\bar{1}2\rangle$ orientation, which is found also for the cold worked regions (Figures. 5.15(c), 5.17(a,b,c) and 5.18(a,b)).

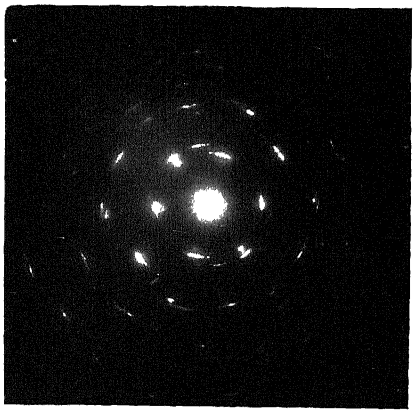

(a) D from region a

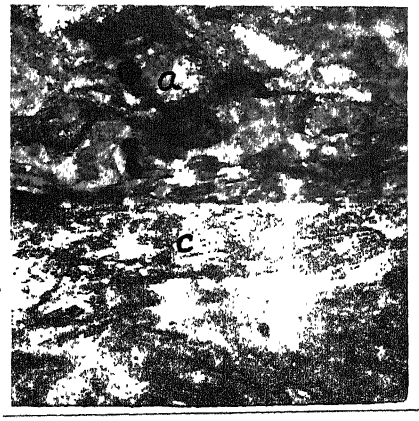

(b) Mag. 7800

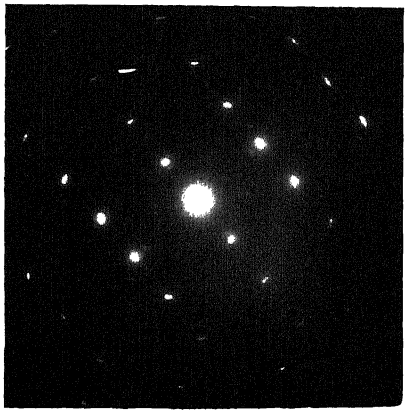

(c) D from region C

Figure 5.14. A typical cold worked area of alloy C consisting of $\{110\}\langle\bar{1}10\rangle$ and $\{112\}\langle\bar{1}\bar{1}D\rangle$ orientations.

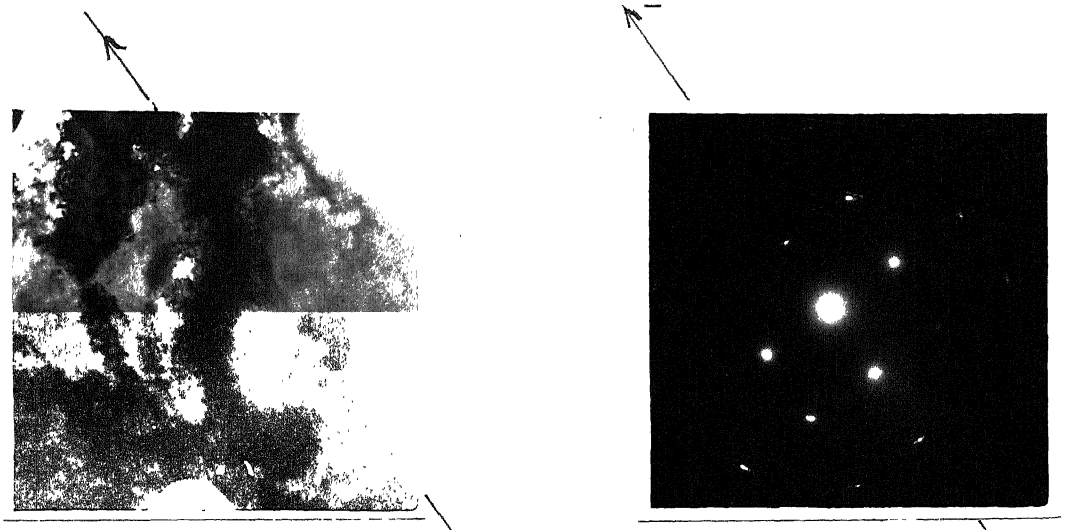

(a) Mag. 20,000. (b)

Figure 5.15. Observation of a cube oriented region in a partially annealed sample at 275°C for 2 hours.

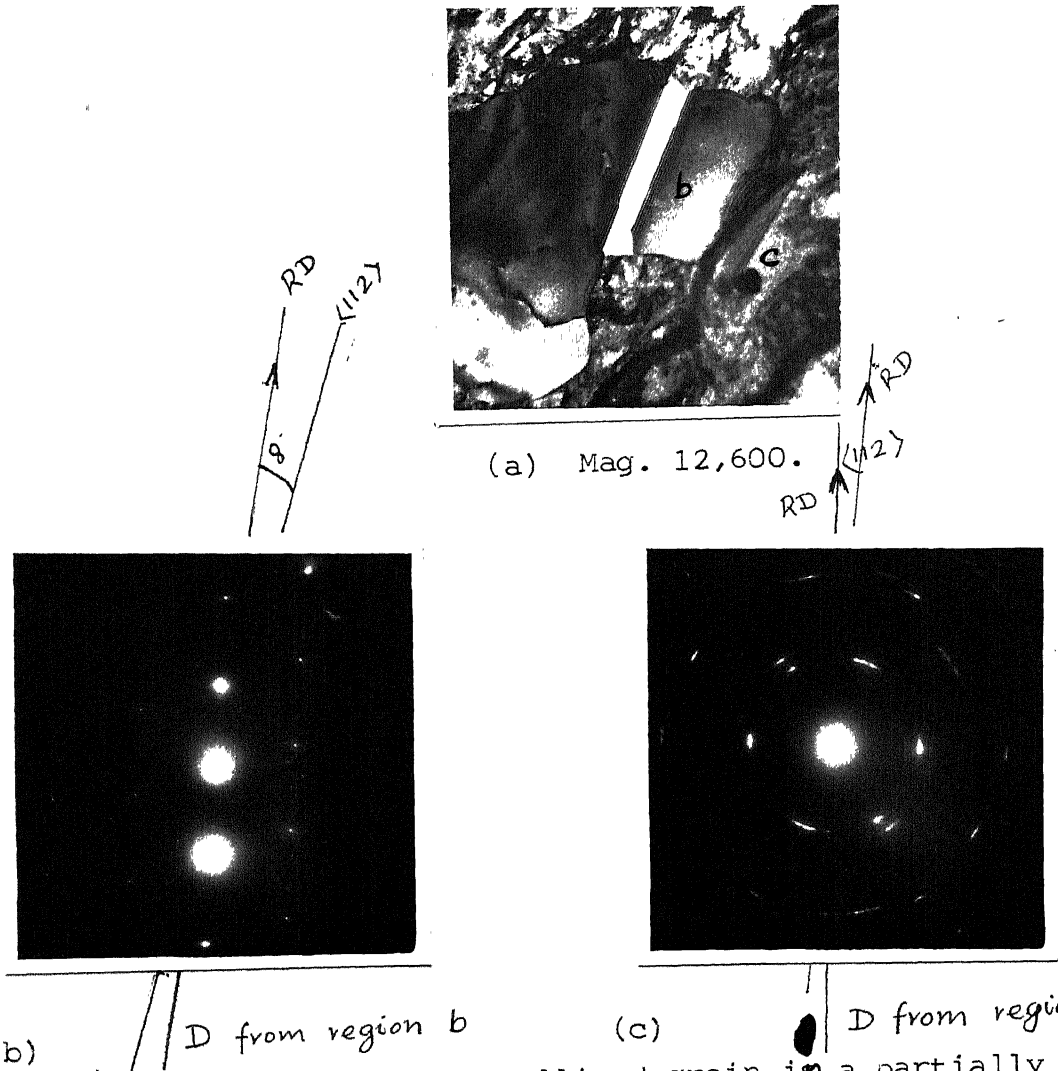

(a) Mag. 12,600.

(b) (c)

Figure 5.16. A well recrystallised grain in a partially annealed sample at 275°C for 2 hours having a closer orientation with the adjacent cold worked matrix.

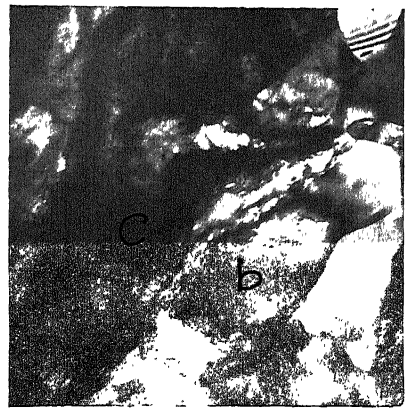

(a) Mag. 26,000.

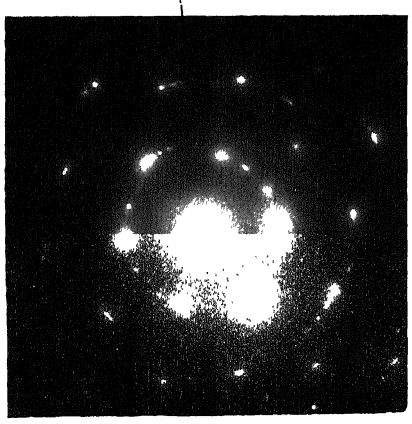

(b) D from region b

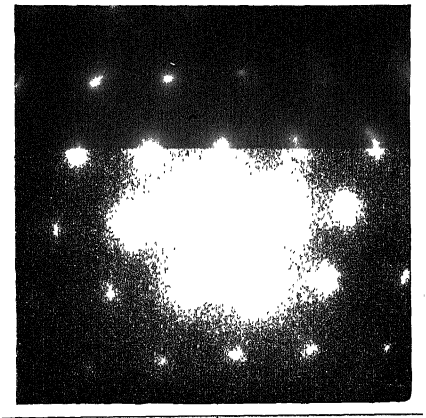

(c) D from region C.

Figure 5.17. A recrystallising nucleus in a partially annealed sample at 275°C for 1 hour having a similar orientation with the cold worked matrix.

(a) Mag. 20,000.

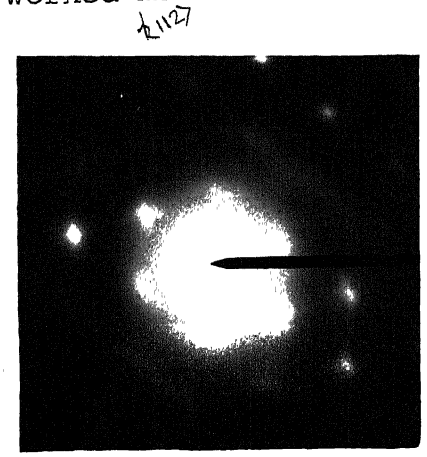

(b)

Figure 5.18. The well recrystallised grain growing into the adjacent cold worked matrix has $\{110\}\ \langle 1\bar{1}2\rangle$ orientation. Sample annealed at 275°C for 5 hours.

5.2.2. Recrystallisation Textures

Figure 5.19 indicates the pole figure of alloy C, which was cold rolled at room temperature and fully recrystallised. It is clear that this pole figure is very similar to pole figure of a 70/30 α-brass. The 70:30 α-brass main texture components have been identified as $\{113\}\langle\bar{2}11\rangle$. The peak pole density in the present pole figure matches quite well with the ideal orientation $\{110\}\ \langle 112\rangle$. This is in agreement with the orientations of the recrystallised grains found in the electron microscopic investigations. However, the present pole figures only give a partial information because the texture for the angular orientation of the specimen corresponding to the peripheral regions of the pole figure was not determined. In the absence of a complete pole figure the texture component cannot be determined with certainty.

Alloy C warm rolled at 100°C followed by full recrystallisation, shows (Figure 5.20) a similar kind of recrystallisation texture as that of alloy C cold rolled at room temperature. Fully recrystallised alloy C, warm rolled at 150°C shows (Figure 5.21) a somewhat different recrystallisation texture, compared to the recrystallised texture of alloy C warm rolled at 100°C. The difference is only in the appearance of a minor texture component, possibly $\{112\}\ \langle 111\rangle$.

5.3. DTA Studies

DTA studies were made on alloy C and pure copper rolled to 95% reduction in thickness, as described in Section 4.6.

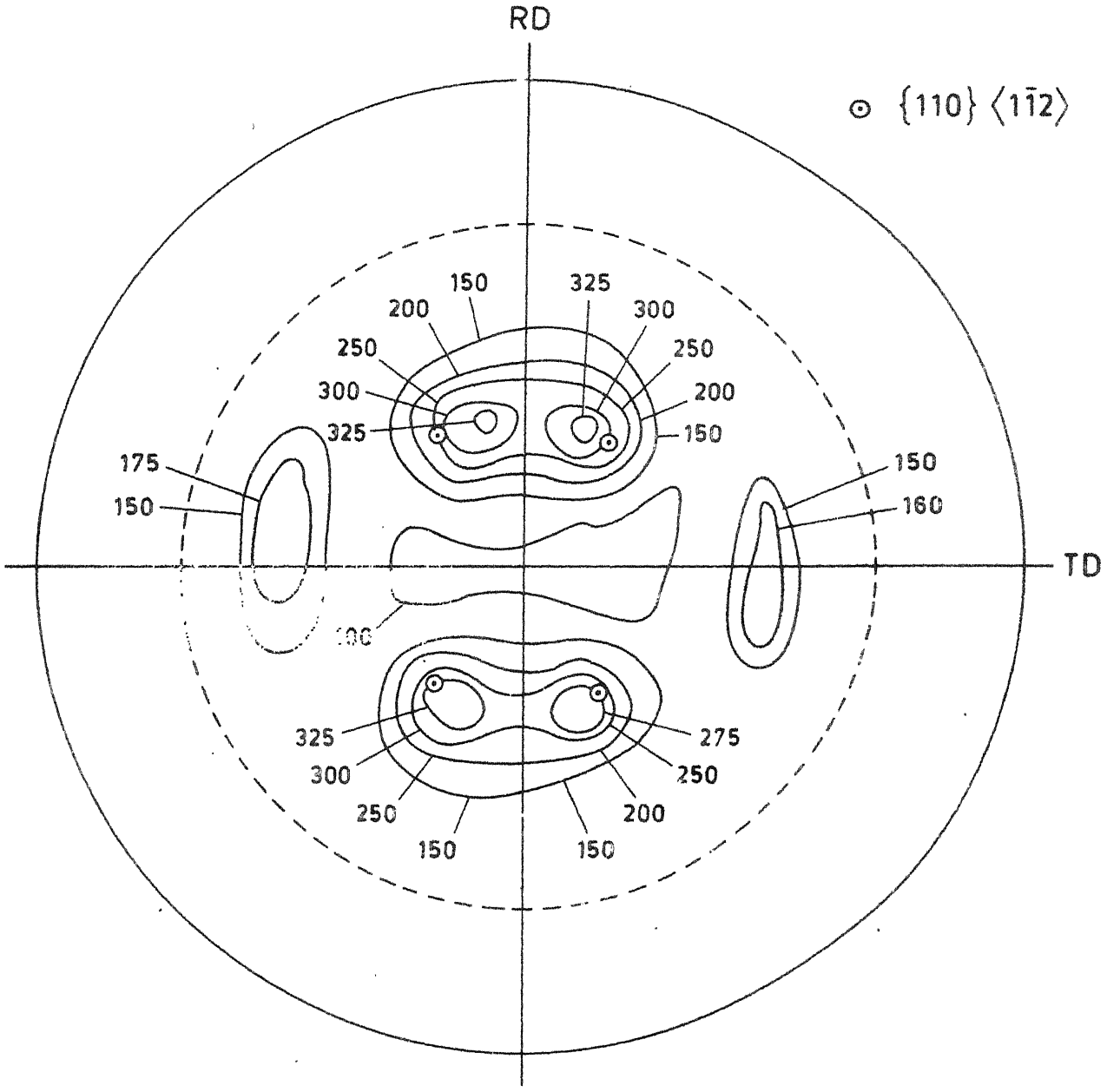

Fig. 5.19. (111) Recrystallisation pole figure of alloy C after coldrolling at room temperature.

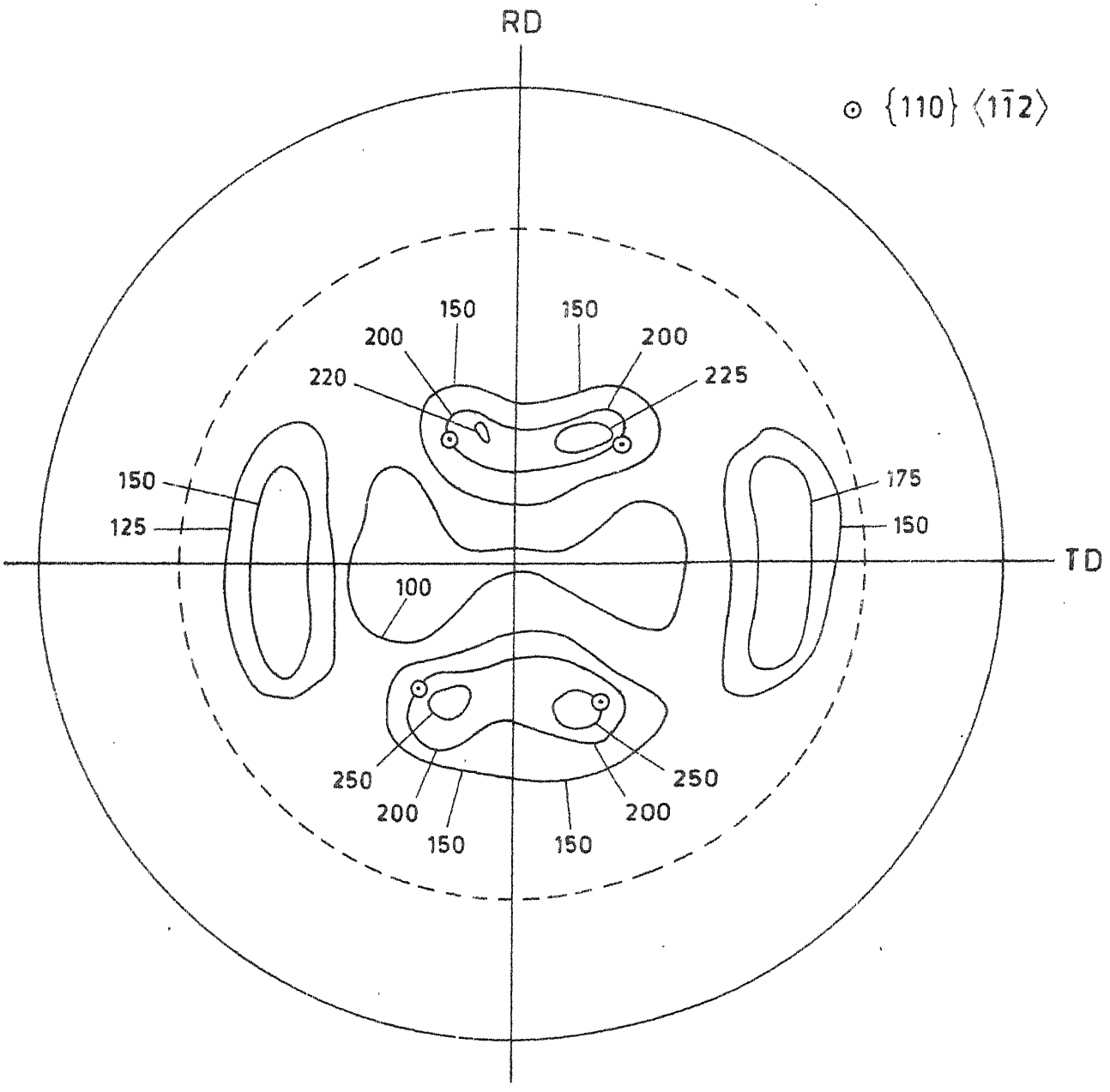

Fig. 5.20. (111) Recrystallisation pole figure of alloy C after warm rolling at 100° C.

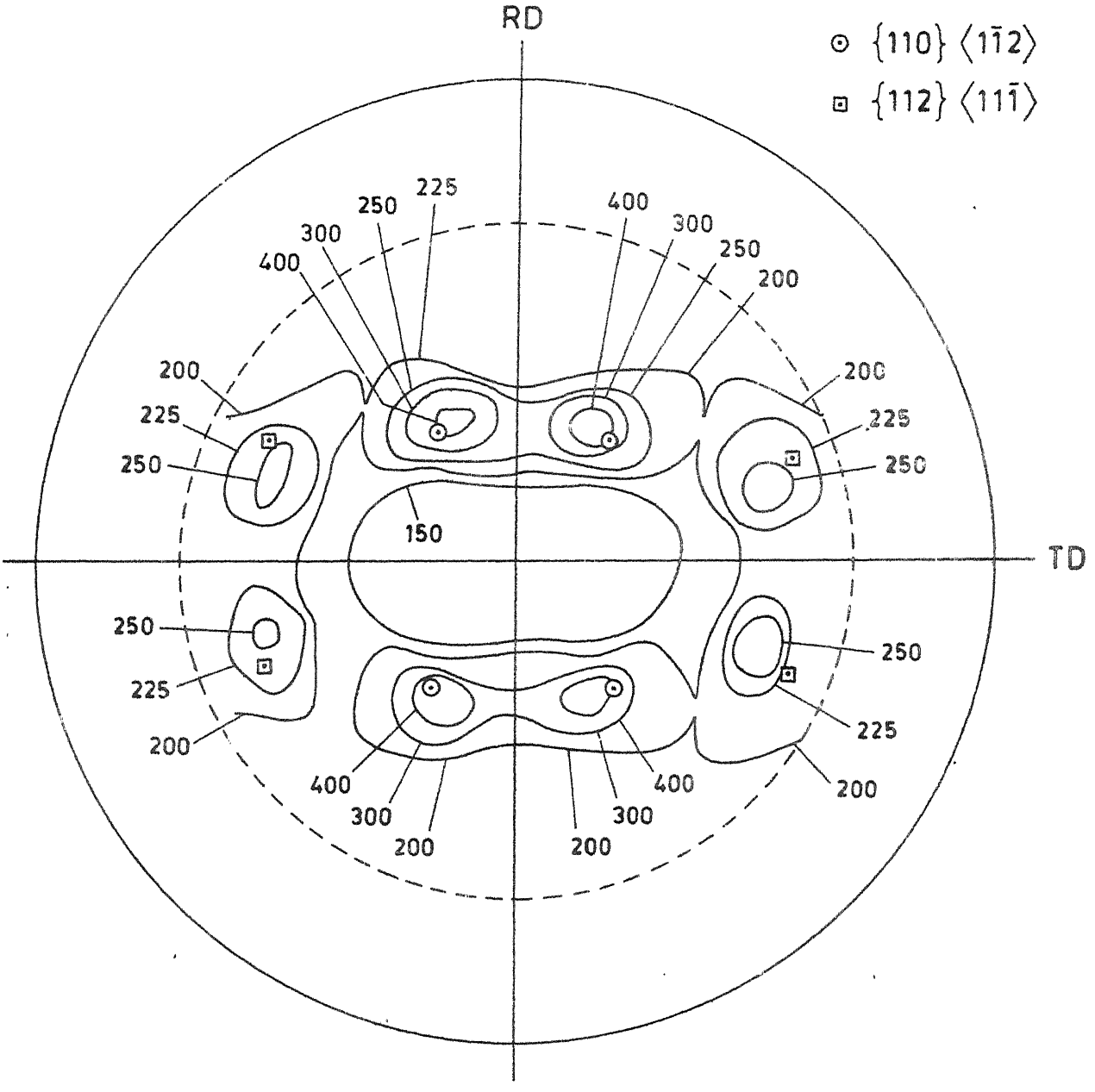

Fig. 5.21. (111) Recrystallisation pole figure of alloy C after warm rolling at 150° C.

Figure 5.22 shows the DTA curves for samples A and C only. It is seen that there are no clean sharp peaks as reported by Byrne[7] and Ray et al.[10] Alloy A virtually does not show any appreciable heat effect, while alloy C shows some heat effect. The main peaks in the DTA traces are absent possibly because the present studies were made $2\frac{1}{2}$ years after rolling the alloys. Probably some amount of stored energy has been already released with time at room temperature which varied between 20°C and 42°C in the whole year. Hence, then thermal effects we see in the present DTA traces are the residual stored energy. If this is considered to be true, then it appears that the Cu-P alloy does not lose stored energy as fast as the pure copper sample.

5.4. Kinetics of Recovery

5.4.1. X-ray Diffraction Technique

To determine the kinetics of recovery of alloy C, peak width method was used. For this purpose, experiments were first conducted in a General Electric XRD-VI X-ray diffractometer. Since for alloys B and D, the (220) reflection had been used to study the change in peak width as a function of annealing time[10], in this investigation also the (220) peak was chosen for the study of recovery kinetics. The (220) reflection from room temperature cold rolled alloy did not show much peak assymetry (Figure 5.23). But when recovery started the (220) peak tended to become assymetric (Figure 5.23). The peak assymetry appears to be probably due to gradual separation of K_{α_1} and K_{α_2} reflections. This indicated that the choice of (220) reflection for the purpose of peak width measurement is not proper.

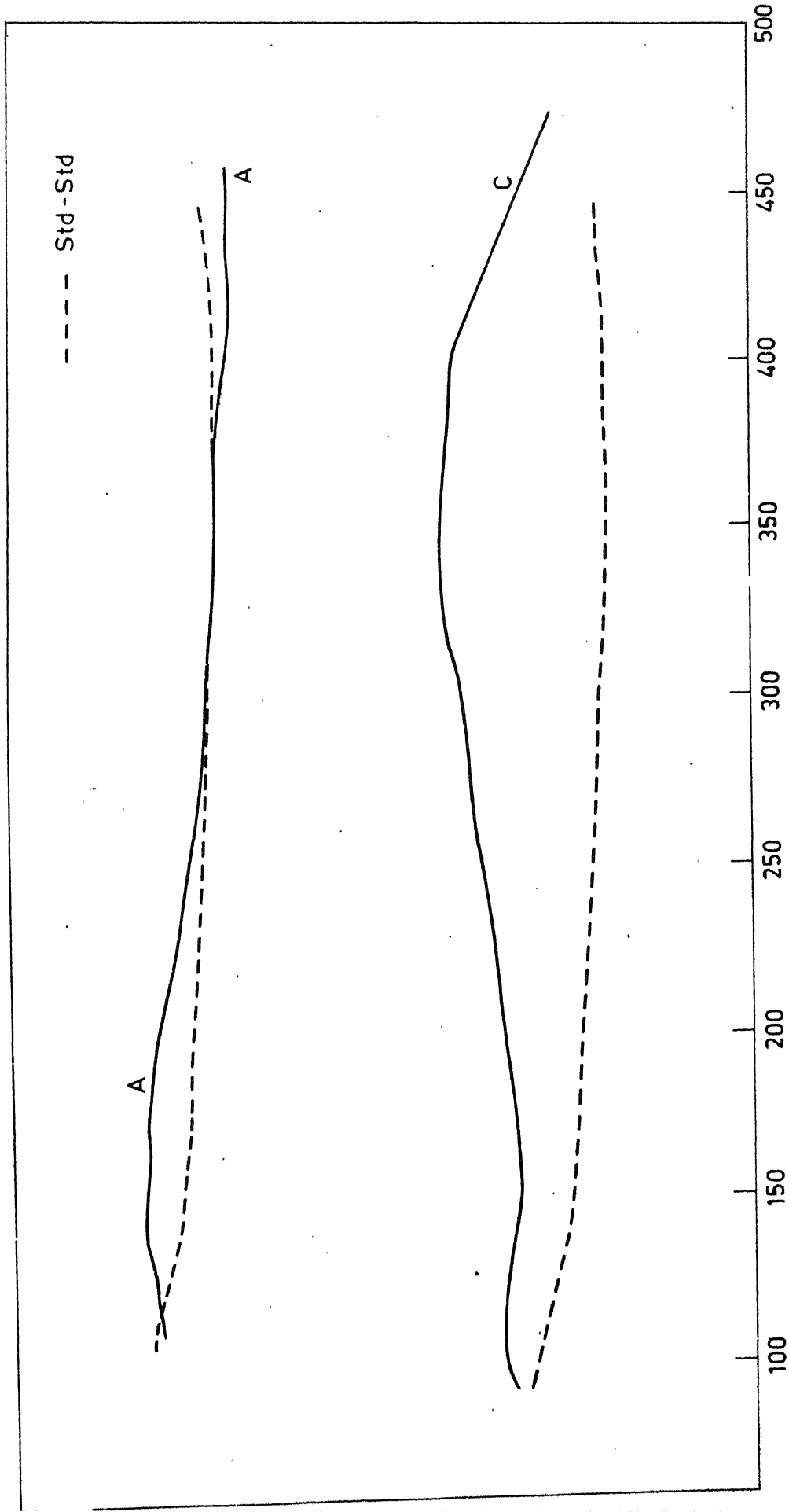

Fig. 5.22. DTA curves for pure copper A and alloy C.

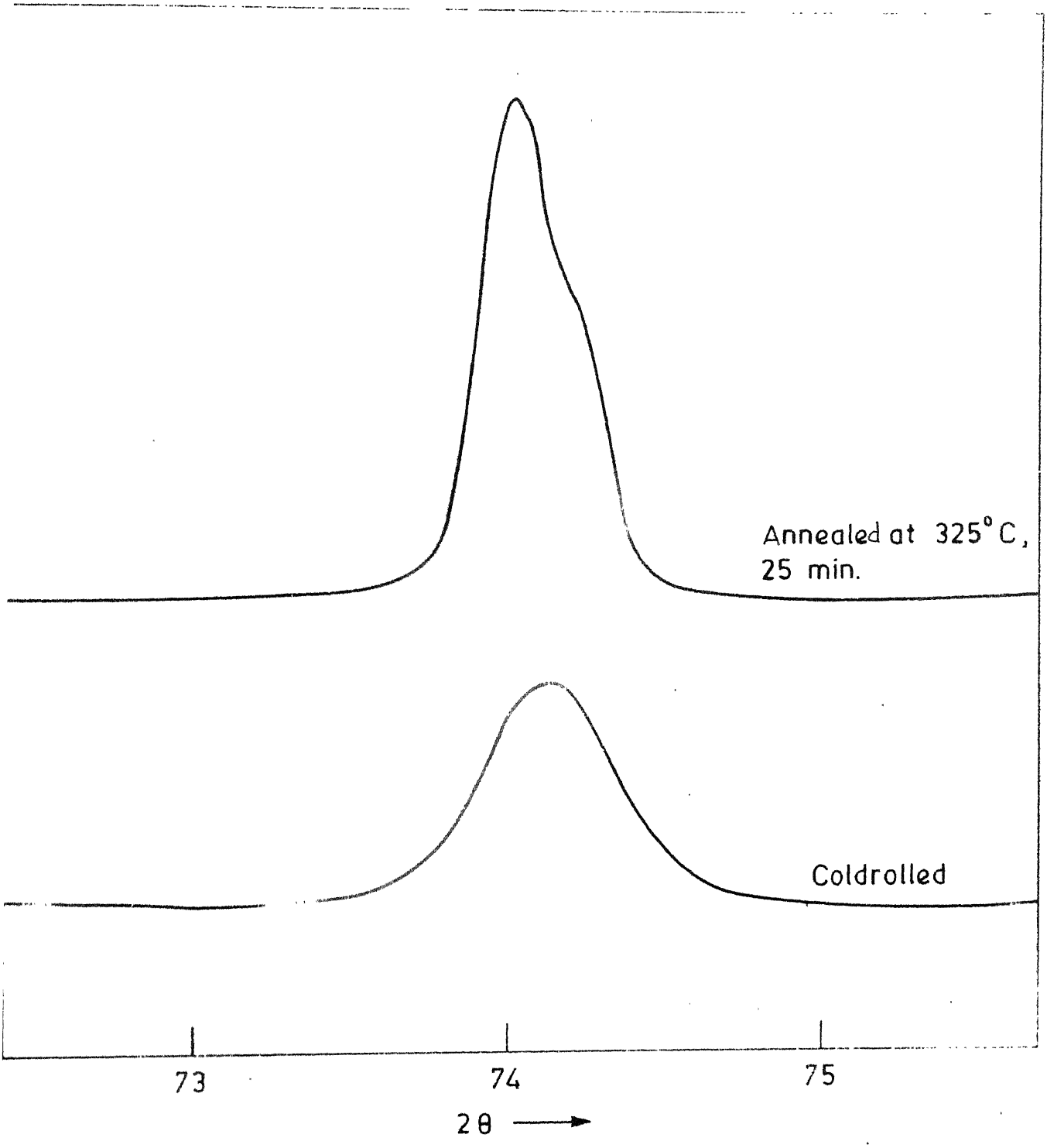

Fig. 5.23. (220) Reflection from alloy C.

In order to generate proper accurate data on peak width, experiments were conducted with Rich-Seifert X-ray diffractometer using the automatic step-scanning mode. From the step-scan data, the peaks were plotted on an enlarged scale. In this experiment, data collected were for the (111), (200) and (220) reflections. Not only (220) reflections showed peak assymetry due to α_1 and α_2 line separation, even (111) reflection showed the same feature but to a lesser extent. Tracing method which gives a more smoothened out curve also did not improve the quality of tne traced peak for the (111) reflection. The more disturbing observations in these experiments was that the peak assymetry did not follow any general pattern (Figure 5.24). Most probably this is due to the fact that for a cold rolled specimen annealing produces grain orientation due to formation of subgrains and small recrystallised grains.of somewhat different orientations causing change in the shape of diffraction peaks. This effect is clearly seen in intensity distributions in pole figures (Figure 5·19). Hence to obtain more uniform peak shape, the specimen was rotated on a rotation stage attached to the GE XRD-VI diffractometer. Even after rotating the sample, the peaks obtained were assymetric, as shown in Figure 5.25. Thus it appears that the study of recovery kinetics of rolled specimen using the X-ray peak breadth method is not a suitable one, because of strong texture and change in texture during annealing.

5.4.2. Resistivity Measurements

Since the X-ray diffraction method failed to yield recovery kinetics data, suitability of 'Electrical Resistivity'

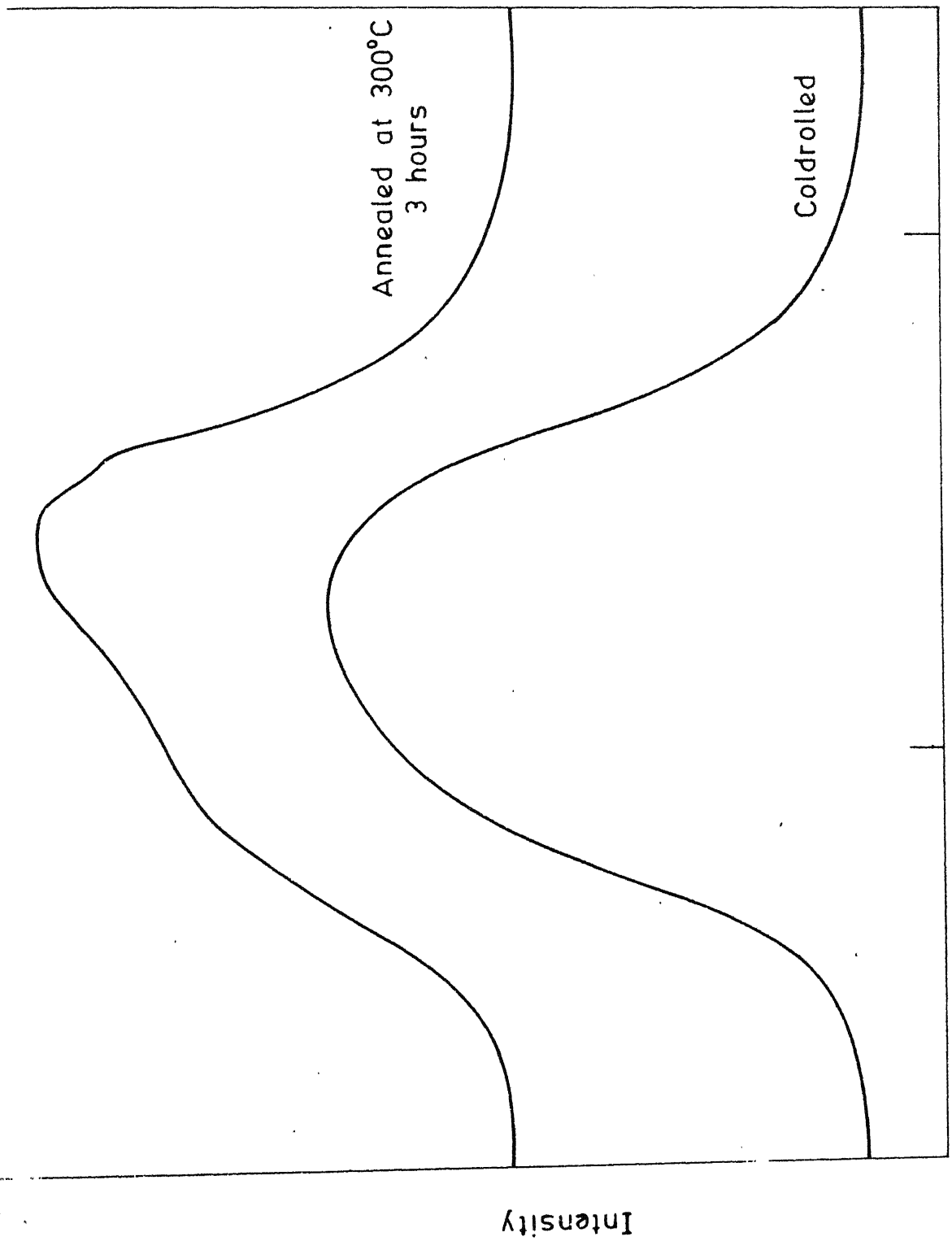

Fig. 5.24. (111) Reflection from alloy C.

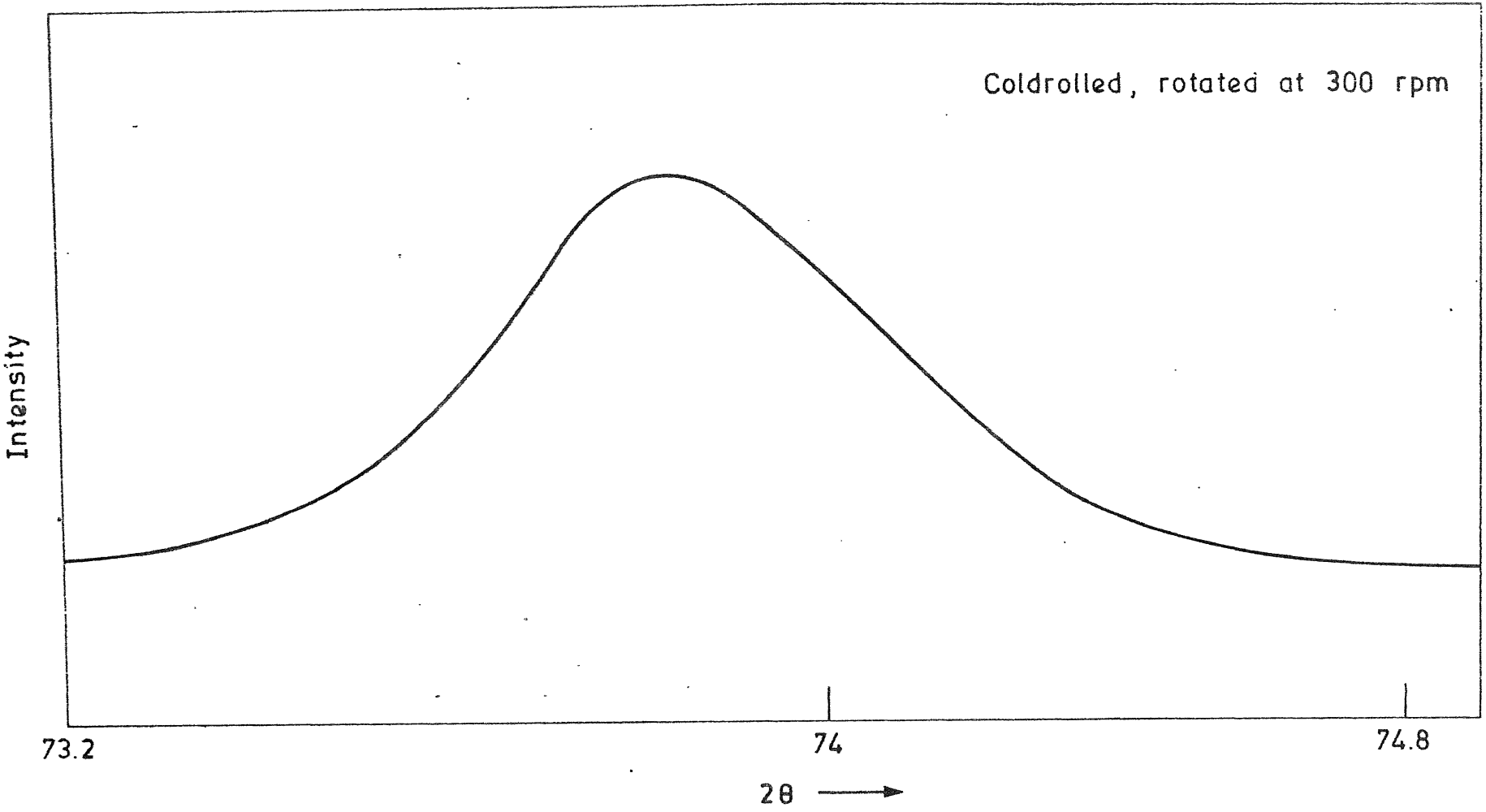

Fig. 5.25. (220) Reflaction from alloy C with sample rotation.

method was tried out. A trial run with cold rolled alloy C specimen kept in silicone oil bath at 275°C showed a general drop of potential (between the potential leads) with annealing time. The change in potential, however, was too small, ~4 μV. Since this change was too small and was of the same order of estimated accuracy, the presently available electrical resistivity set up was not found suitable to yield reliable results. The silicone oil deteriorated very rapidly at around 300°C. No suitable bath was also possible to find to cover the entire range of temperatures of interest, namely 275°C to 325°C.

5.5. Kinetics of Recrystallisation

Fraction recrystallised was found out by the usual point counting method, applied on the enlarged photomicrographs. Two representative photographs are shown in Figures 5.26 and 5.27. The recrystallisation data are shown in Table 5.1,,and the fraction recrystallised vs. log time plots for three different annealing temperatures are shown in Figure 5.28. From this plot, time for 50% recrystallisation vs. corresponding $(\text{Temperature})^{-1}$ was plotted, which yielded a straight line plot as shown in Figure 5.29. The exponential law

$$\text{Rate} = A \exp(-Q/RT) \qquad (5.1)$$

where A is a constant, a is activation energy for recrystallisation, T is absolute temperature and R is gas constant, is thus applicable. The slope of the straight line gives Q/R. The activation energy Q for recrystallisation was found to be

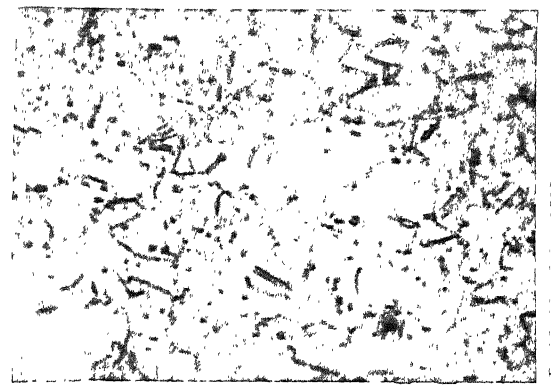

Figure 5.26. Microstructure of alloy C annealed at 325°C for 2 hours. Mag. 2440.

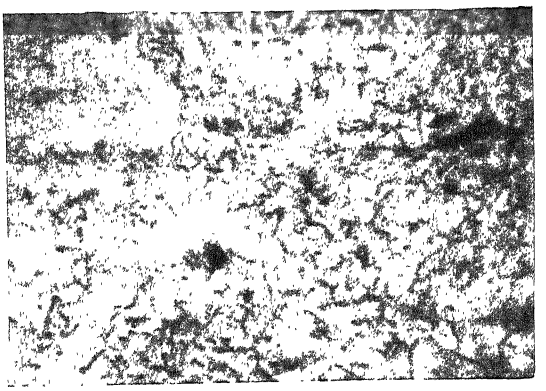

Figure 5.27. Microstructure of alloy C annealed at 325°C for 30 minutes. Mag. 2440.

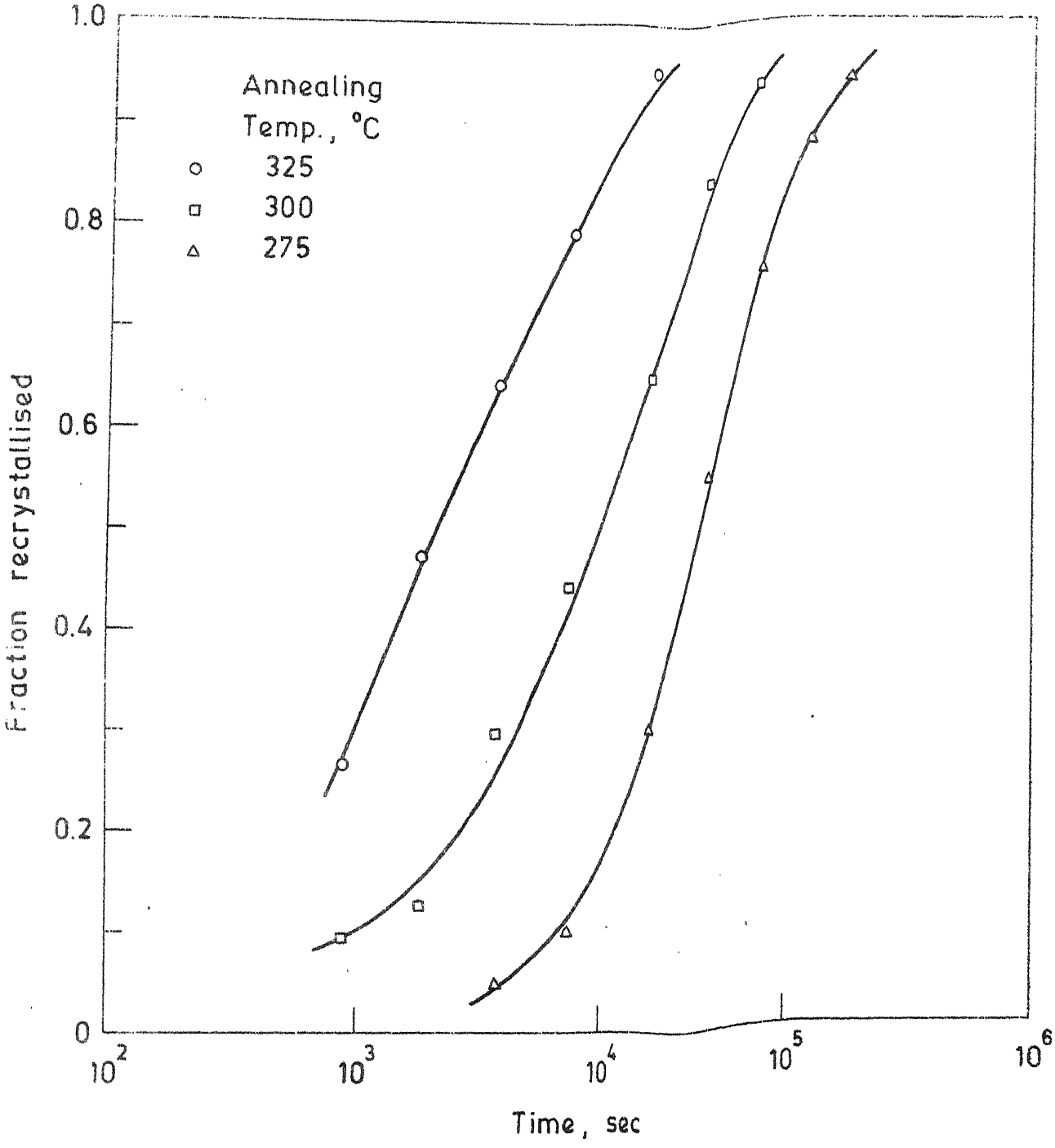

Fig. 5.28. Variation of fraction recrystallised with annealing time.

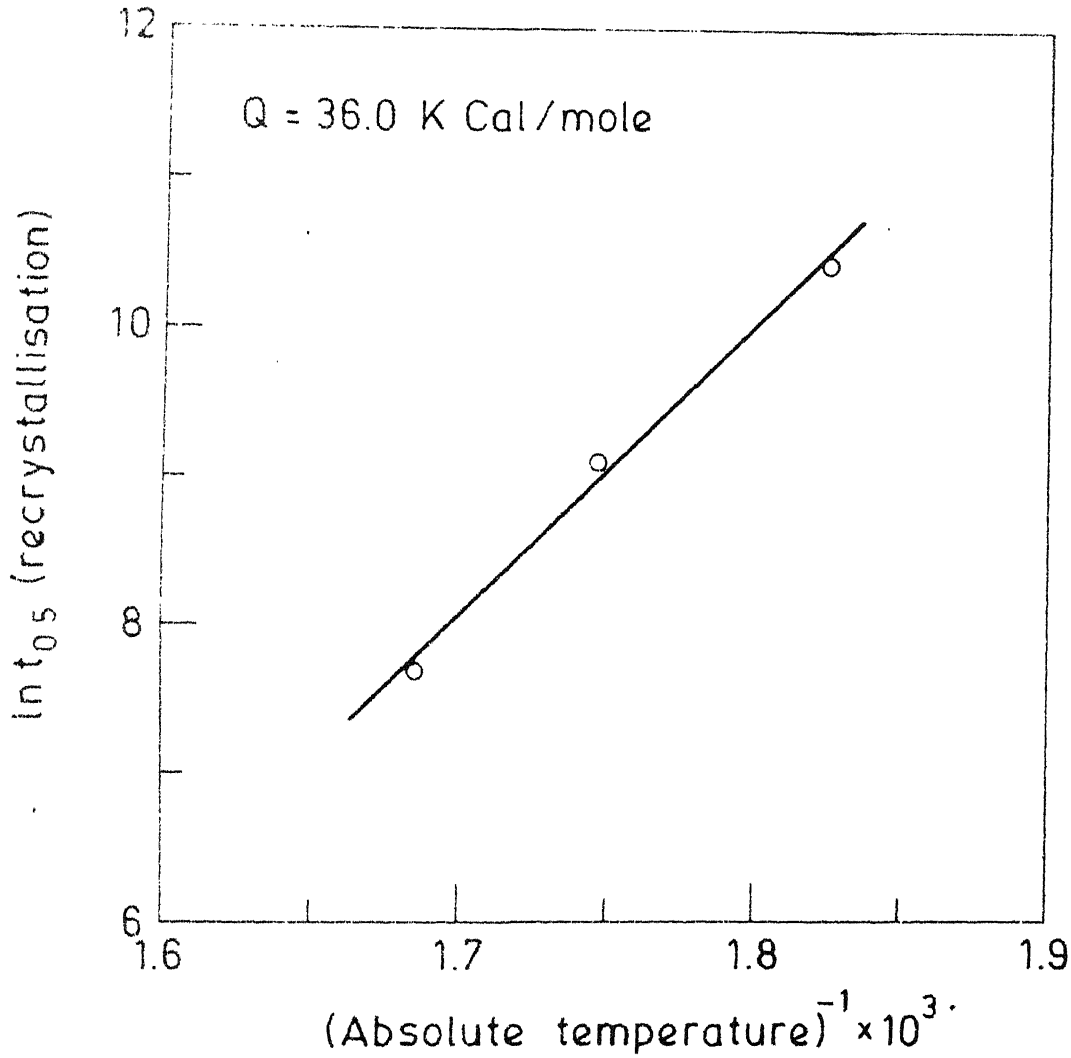

Fig. 5.29. Variation of annealing time for 50 % recrystallisation with temperature.

36 KCal/mole. This value matches very well with the activation energy for recrystallisation found for alloys B and D, which are about 35 KCal/mole.[10]

Table 5.1. Percent Recrystallisation at Different Temperatures with Time for Alloy C

Temperature, °C / Time	% recrystallised grains at temperatures		
	325°C	300°C	275°C
5 min	-	-	-
15 min	26.0	10.0	-
30 min	47.66	12.5	-
60 min	64.3	29.0	5.0
2 hours	80.0	42.0	10.0
5 hours	95.0	65.0	30.0
10 hours	-	84.0	55.0
20 hours	-	95.0	75.0
36 hours	-	-	88.0
50 hours	-	-	95.0

CHAPTER 6

DISCUSSIONS

6.1. Recrystallisation Behaviour

From the TEM studies on the deformed state of all the five alloys, we see that alloys A, B and C have cube oriented regions in the deformed matrix itself, while no such cube oriented regions could be seen in alloys D and E. Since alloys D and E contain higher amount of phosphorous, it appears that the existence of cube oriented regions in the deformed matrix depends on the amount of alloying element present. Since alloying Cu with Al, Si, P etc. lowers the stacking fault energy rather drastically to lower values[39] it may be said that very low stacking fault energy of a material does not favour formation of cube oriented regions. The occurrence of more number of twins in specimens D and E can also be attributed to very low stacking fault energy of the alloys.

Annealing studies of cold rolled alloy has shown that some cube oriented regions are still present in the just started to recrystallise samples. But these cube oriented regions did not show any sign of forming recrystallised regions. The difficulty of formation of cube recrystallised grains may be explained in the following way.

Ray et al.[10] have found from DTA studies that increase in alloying content increases the stored energy in the material. They have also found out that the release of stored energy is slower in higher phosphorous content alloys compared to pure

copper. In the present investigation also, it is found that alloy C has got more residual stored energy than pure copper. These observations suggest that the recovery process is slower in alloy C compared to pure copper. The slow recovery process for the phosphorous containing alloys suggests that the rearrangement of dislocations is hampered due to the presence of phosphorous atoms. For a high angle grain boundary to form, rearrangement of dislocations is necessary. Since these dislocations cannot move easily in Cu-P alloys, a recrystallising nuclei with high misorientations with the adjacent matrix cannot form easily. Hence this may explain the absence of cube oriented nuclei in alloys D and E and in annealed alloy C.

In the same annealed sample, where the cube oriented regions were seen, some well recrystallised grains were also detected. These recrystallised regions, however, do not have the cube orientation. It is found that these well recrystallised grains have the orientation $\{110\}\langle 112\rangle$ or near to it. It is also seen that the well recrystallised grains appears to have the same or very close orientation relative to the adjacent cold worked matrix. Thus, it appears that the cube oriented regions, even if they are present, do not grow, instead the recrystallised grains with orientation similar to the adjacent cold rolled matrix grow. This behaviour can possibly be justified in terms of Lucke and Deterts[11] solute drag mechanism.

Cube grains have a high misorientation with the adjacent cold worked matrix. The boundary regions between the cube

oriented regions and the matrix is thus a region of high degree of misorientation and is possibly similar to a high angle grain boundary. According to Lucke and Deterts[11], the impurity atoms in solid solutions tend to segregate to such high angle grain boundaries. When such a boundary laden with impurity atoms start migrating, a drag is created by the impurity atmosphere, which may compel the boundary to carry the impurity along with it. In this case the boundary movement is impeded by the segregated solute atoms. This is the so-called solute drag theory of Lucke and Deterts.[11]

A small subgrain or a recrystallised grain with high degree of misorientations with the adjacent deformed matrix, like the cube oriented region in the deformed matrix, may start moving fast into the adjacent cold worked matrix in alloy C. The phosphorous content of such a boundary may increase with the distance traversed and hence the boundary velocity is expected to decrease due to the solute drag effect. A stage may reach soon when the boundary becomes completely immobile and further recrystallisation will be possible only through the formation of new nuclei within the deformed matrix. Since regions bounded by high angle boundaries become immobile, the growth of those nuclei having small misorientation relative to the deformed matrix may grow fast and finally engulp the cube grains. This process appears to occur, as has been seen by Ray et al.[40] in their dynamic recrystallisation studies of alloy B through HVEM.

The recrystallisation kinetics of alloy C has shown a boundary migration activation energy of 36 KCal/mole. This is

higher than that of pure copper, but is lower than the activation energy for self diffusion of Cu. This may be expected. In the recrystallisation process boundary migration is due to jump of atoms from the deformed matrix to the recrystallised grain. The jump involves an activation energy. The jump of an atom across the boundary is expected to involve less activation energy than jump of an atom from a lattice site to a vacant site within the lattice because the atoms are less densely packed at the boundary. The activation energy of self diffusion of Cu is ~47 KCal/mole. The low value of boundary migration activation energy of 20 KCal/mole has been determined for recrystallisation on pure copper[10] is in agreement with the assumptions made above. In Cu-P alloy, however, phosphorous segregates at the boundary. Thus a grain boundary will be bound to a phosphorous atom. If the boundary tries to move leaving the phosphorous atom extra energy is expected to be involved and this should raise the activation energy of boundary migration compared to pure Cu. The observed value of 36 KCal/mole activation energy thus appears to be a reasonable activation energy for boundary migration for Cu-P alloy.

6.2. Textures

Ray et al.[41] have studied recrystallisation behaviour of pure copper using HVEM. This dynamic study of recrystallisation of copper shows that cube oriented subgrains present in cold worked matrix of pure copper, recrystallises fast and grows at the expense of cold worked matrix resulting in cube oriented grains, or cube texture. However it was found that if sample

prepared for electron microscopic studies did not contain any cube subgrains in the cold worked matrix, then the other subgrains grew to large size and no cube oriented grain was produced. This shows that in pure copper presence of cube oriented subgrain is a necessary condition for the development of cube texture.

Though cube oriented regions are present in the cold worked matrix of alloy C, still cube texture is not obtained. This is possibly because of the solute drag effect as explained before.

Hu et al.[4] have concluded from their studies in stainless steel, that for a cube annealing texture to be formed, the starting deformation texture should be sharp pure metal type texture. Even though, alloy C after warm rolling at 100°C produced a considerably sharp copper type rolling texture, it did not give rise to a cube recrystallisation texture. In fact, there is practically no difference between the (111) recrystallisation texture pole figures obtained with room temperature cold rolled and 100°C warm rolled alloy C. The recrystallisation texture pole figures resemble closely with that of 70/30 α-brass recrystallisation texture.

The annealing texture pole figure for 150°C warm rolled alloy C appears somewhat different compared to the annealing textures obtained with the alloy cold rolled at room temperature and warm rolled at 100°C. The major difference is in the change in minor texture component (possibly $\{225\}\langle 73\bar{4}\rangle$) to a new minor texture component which appears to be $\{112\}\langle 11\bar{1}\rangle$.

Development of texture has been related to the stacking fault energy.(SFE).[42] Nickel has a high SFE, 250 ergs/cm^2.[43] Additions of Fe or Cu, does not change the SFE appreciably. The observation of a not so sharp a cube texture in Ni - 20% Fe - 5% Cu alloy possibly is related to the high stacking fault energy of the alloy.[44] Since Ti is known to drastically reduce the stacking fault energy of Ni, small additions of Ti ($\sim$2 at. %) was made in Fe-Ni-Cu alloy and very sharp cube texture could be produced.[44] Copper has a moderate stacking fault energy $\sim$ 5 5 ergs/cm^2 and very sharp cube texture can be produced in pure Cu. On the other hand, additions of alloying elements like Zn, Al, P etc. lowers the stacking fault energy of Cu, the rate of decrease is more with increase in the valence of solute element. For the alloy composition under consideration the stacking fault energy is very low $\sim$ 5 ergs/cm^2. All these alloys do not show sharp copper type rolling texture, and no cube texture is formed. From this observations it appears that cube nuclei have a tendency to grow if the SFE lies within a favourable band of SFE values, which is possibly centred around copper. Raising stacking fault energy of a low SFE material may induce in it a favourable growth of cube oriented regions. It is known that stacking fault energy increases in many materials with increase in temperature.[39] It has been observed that stainless steel, which has a low stacking fault energy $\sim$20 ergs/cm^2, on warm rolling at $\sim$800°C produces on annealing a sharp cube texture, even though room temperature rolling of stainless steel does not produce cube texture.[45] This may indicate a strong influence of stacking fault energy on the growth of cube oriented grains. However, the

correlation is qualitative, as the exact relationship between the stacking fault energy and recrystallisation behaviour is not known. This qualitative picture gives another possible explanation why in Cu-P alloy cube oriented subgrains do not grow. At the present time, it is not clearly known whether the solute drag effect approach is more appropriate or the stacking fault energy concept is more appropriate for the growth of cube oriented grains.

CHAPTER 7

CONCLUSIONS

Several conclusions can be drawn from the present investigation.

(i) The availability of cube oriented regions in the deformed matrix seems to depend heavily on the amount of solute element content and hence possibly on stacking fault energy.

(ii) Alloying copper with phosphorous retard the recrystallisation process.

(iii) No cube texture was obtained on annealing room temperature cold rolled or warm rolled Cu-P alloy.

(iv) It appears that the recrystallised grains, which have similar orientation relative to the deformed matrix grow fast to give rise to a pronounced brass type.

(v) Room temperature rolling of alloy C did not give rise to a sharp copper type texture. By warm rolling of alloy C at 100°C sharper copper type texture could be produced.

(vi) It appears that the study of recovery kinetics of rolled specimen using the X-ray peak breadth method is not a suitable one.

CHAPTER 8

SUGGESTIONS FOR FURTHER WORK

Recrystallisation studies can be made on alloys that may produce a second phase on annealing, such that the effect of the second phase on recrystallisation behaviour can be studied. For example, alloy E, for which the composition range is in the second phase region, annealing of this alloy may give rise to Cu_3P precipitation. Effect of this precipitation on annealing behaviour of alloy E can be studied.

From the present investigation, it is seen that warm rolling of alloy C at 100°C produced sharp copper type rolling texture and the sharpness has diminished when the alloy was rolled at 150°C. So a rolling temperature in between 100° and 150°C may be tried which may lead to sharper copper type texture. Electron microscopic studies should be done on warm rolled state and annealed state of the alloys, to understand the effect of warm rolling on recrystallisation behaviour.

REFERENCES

1. J.G. Byrne, 'Recovery, Recrystallisation and Grain Growth', p. 1, The Macmillan Co., New York (1965).

2. J.E. Bailey and P.B. Hirsh, Proc. Roy. Soc. A267, 11 (1962).

3. S. Weissmann, T. Imura and W. Hosokawa, 'Recovery Recrystallisation of Metals', Ed. L. Himmel, p. 241, Interscience, New York (1963).

4. H. Hu, R.S. Cline and S.R. Goodman, 'Recrystallisation, Grain Growth and Textures', p. 295, ASM, Metals Park, Ohio (1966).

5. F. Haessner, 'Recrystallisation of Metallic Materials', Ed. F. Haessner, p. 5, Dr. Riederer-Verlag, Stuttgart (1971).

6. L.M. Clarebrough, M.E. Hargreaues and M.H. Loretto, Acta Met., 8, 797 (1960).

7. J.G. Byrne, 'Recovery, Recrystallisation and Grain Growth', p. 37, The Macmillan Co., New York (1965).

8. H. Hu, Trans. AIME, 75, 224 (1962).

9. R.W. Cahn, J. Inst. of Metals, 76, 121 (1949).

10. R.K. Ray and W.B. Hutchinson, Proc. of Conf. on Recrystallisation in the Development of Microstructure', Metal Science, 13, 125 (1979).

11. K. Lücke and K. Detert, Acta Met., 5, 628 (1957).

12. M. Hillert, Proc. of Conf. on Recrystallisation in the Development of Microstructure, Metal Science, 13, 118 (1979).

13. A.R. Jones, B. Ralph and N. Hansen, Proc. of Conf. on Recrystallisation in the Development of Microstructure, Metal Science, 13, 149 (1979).

14. J.G. Byrne, 'Recovery, Recrystallisation and Grain Growth', p. 71, The Macmillan Co., New York (1965).

15. P.A. Beck and P.R. Sperry, Ja. Appl. Phys., 21, 150 (1950).

16. I.L. Dillamore, P.L. Morris, C.J.E. Smith and W.B. Hutchinson, Proc. Roy. Soc., A239, 405 (1972).

17. K.T. Aust and J.W. Rutters, 'Recovery and Recrystallisation of Metals', Ed. L. Himmel, p. 131, Interscience, New York (1963).

18. R.W. Rath and H. Hu, Trans. AIME, 215, 119 (1959).

19. R.W. Cahn, 'Physical Metallurgy', Ed. R.W. Cahn, p. 960, North Holland, Amsterdam (1965).

20. R.K. Ray and W.B. Hutchinson, Phil. Mag., 28, 831 (1973).

21. B.D. Cullity, 'Elements of X-ray Diffraction', p. 285, Addison-Wesley, Reading, Mass. (1956).

22. H.J. Bunge and F. Heassner, J. Appl. Phy., 39, 5503 (1968).

23. F.A. Underwood, 'Textures in Sheet Metals', p. 2, MacDonald, London (1961).

24. F. Haessner, Z. Metallkunde, 54, 98 (1963).

25. R.E. Smallman, J. Inst. of Metals, 84, 10 (1955-56).

26. R.E. Smallman and D. Green, Acta Met., 12, 145 (1964).

27. K. Wierzbanowski, 'Texture of Metals', Ed. G. Gottstein and K. Lucke, Proc. of 5th Int. Conf., Vol. I, p. 309, Springer-Verlag, Berlin (1978).

28. C.S. Barret and T.B. Massalski, 'The Structure of Metals', McGraw Hill, New York (1968).

29. A. Merlini and P.A. Beck, Trans. AIME, 203, 385 (1955).

30. R.H. Richman and Y.C. Liu, Trans. AIME, 221, 720 (1961).

31. R.K. Ray, 'An HVEM Study of Recrystallisation in Copper Alloys', Ph.D. Thesis, Submitted at the University of Birmingham, Aston, Birmingham (1973).

32. Y.C. Liu and W.R. Hibbard, Jr., Trans. AIME, 197, 257 (1954).

33. C.S. Barrett, Trans. AIME, 137, 128 (1940).

34. H.W.T. Heller, J.W.H.G. Slakhorst and C.A. Varbaak, 'Texture of Metals', , Ed., Gottstein and K. Lücke, Proc. of 5th Int. Conf., p. 501, Springer-Verlag, Berlin (1978).

35. P. Herbst and J. Huber, 'Texture of Metals', Ed. Gottstein and K. Lücke, Proc. of the 5th Int. Conf., p. 453, Springer-Verlag, Berlin (1978).

36. Gerhard Ibe, 'Texture of Metals', Ed., Gottstein and K. Lücke, Proc. of the 5th Int. Conf., p. 491, Springer-Verlag, Berlin (1978).

37. S. Naka, R. Pennelle, R. Valle and P. Cacombe, 'Texture of Metals', Ed., Gottstein and K. Lücke, Proc. of the 5th Int. Conf., p. 405, Springer-Verlag, Berlin (1978).

38. R.K. Ray and W.B. Hutchinson, Phil. Mag., 28, 953 (1973).

39. R.E. Reed-Hill, 'Physical Metallurgy Principles', p. 20, East-West Publishers, New Delhi,(1973).

40. R.K. Ray and W.B. Hutchinson, Acta Met., 23, 83 (1975).

41. R.K. Ray and W.B. Hutchinson, J. Microscopy, 97, 217 (1973).

42. G. Wassermann, Z. Metallkunde, 54, 836 (1960).

43.

44. V.S. Verma, 'Study of Process Variables on the Development of Cube Texture in Copper Bearing Soft Magnetic Fe-Ni Alloys', M.Tech. Thesis, Submitted at I.I.T. Kanpur (1981).

45. H. Hu, Trans. AIME, 194, 83 (1952).

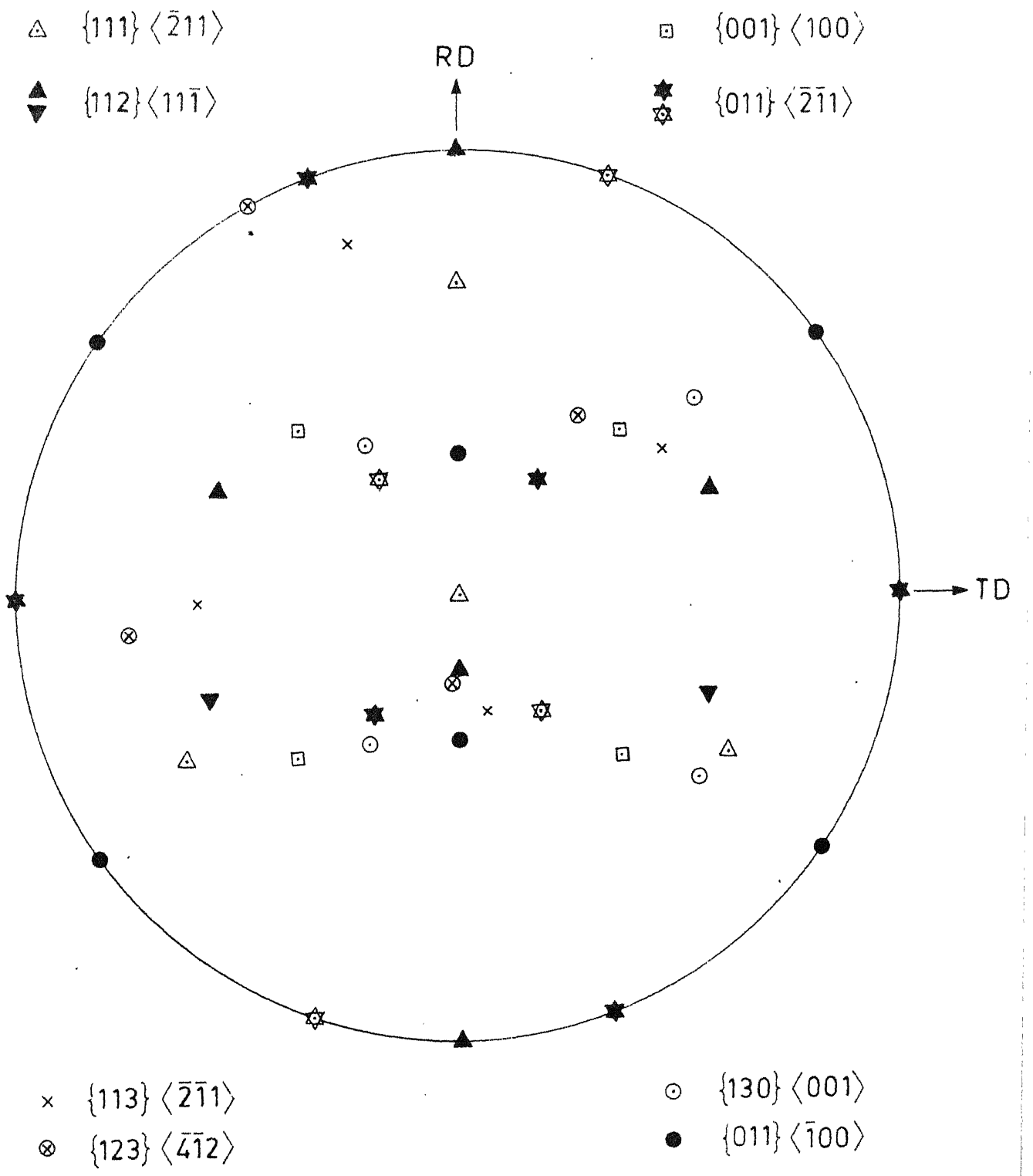

Standard (111) pole figure showing ideal pole locations.